



Article

# Method for Determining the Degree of Damage to the Stator Windings of an Induction Electric Motor with an Asymmetric Power System

Juraj Gerlici <sup>1</sup>, Sergey Goolak <sup>2</sup>, Oleg Gubarevych <sup>3</sup>, Kateryna Kravchenko <sup>1</sup>,\*, Kateryna Kamchatna-Stepanova <sup>4</sup> and Andrey Toropov <sup>5</sup>

- Department of Transport and Handling Machines, University of Žilina, Univerzitná 8215/1, 010 26 Žilina, Slovakia; juraj.gerlici@fstroj.uniza.sk
- Department of Electromechanics and Rolling Stock of Railways, State University of Infrastructure and Technologies, Kyrylivska Str., 9, 04071 Kyiv, Ukraine; gulak\_so@gsuite.duit.edu.ua
- Department of Navigation and Operation of Technical Systems on Water Transport, State University of Infrastructure and Technologies, Kyrylivska Str., 9, 04071 Kyiv, Ukraine; oleg.gbr@ukr.net
- Department of Mechanical Engineering Technology and Metal-Cutting Machines, National Technical University (Kharkiv Polytechnic Institute), Kyrpychova Str., 2, 61002 Kharkiv, Ukraine; kateryna.kamchatna@khpi.edu.ua
- Department of Electrical Engineering, Volodymyr Dahl East Ukrainian National University, Prospect Tsentralnyiy 59a, 93400 Severodonetsk, Ukraine; toropov@snu.edu.ua
- \* Correspondence: kateryna.kravchenko@fstroj.uniza.sk

**Abstract:** A method is proposed for determining the number of damaged stator windings in the presence of an asymmetric power supply system for an induction electric motor based on the Park vector hodograph. As a result of the experiments on the simulation model, it was found that with the symmetry of the system of supply voltages and stator windings, the hodograph of the Park vector describes a circle; in all other cases it is an ellipse. It has been established that the presence of asymmetry in the supply voltage system is indicated by the angle of inclination of the ellipse, and the indicator of the presence of the asymmetry of the stator windings is the angle of ellipticity. In order to identify the presence of asymmetry of the stator windings in the conditions of asymmetry of the supply voltage system, an algorithm for recalculating the ellipse parameters for the condition of the symmetry of the supply voltage system was proposed. Recalculation errors did not exceed 6%. It has been established that the dependence of the increment of the amplitudes of the phase and angles of the phase currents of the stator on the number of damaged turns of the stator winding is linear. Based on this fact, an algorithm for determining the number of damaged turns was proposed. The results of this work can be used to build systems for diagnosing the interturn short circuit of the stator of an induction electric motor built into the drive.

Keywords: induction motor; interturn circuit; asymmetry of the power system; Park vector

## check for updates

Citation: Gerlici, J.; Goolak, S.; Gubarevych, O.; Kravchenko, K.; Kamchatna-Stepanova, K.; Toropov, A. Method for Determining the Degree of Damage to the Stator Windings of an Induction Electric Motor with an Asymmetric Power System. *Symmetry* 2022, 14, 1305. https://doi.org/10.3390/ sym14071305

Academic Editor: Luca Paolo Ardigo

Received: 18 May 2022 Accepted: 19 June 2022 Published: 23 June 2022

**Publisher's Note:** MDPI stays neutral with regard to jurisdictional claims in published maps and institutional affiliations.



Copyright: © 2022 by the authors. Licensee MDPI, Basel, Switzerland. This article is an open access article distributed under the terms and conditions of the Creative Commons Attribution (CC BY) license (https://creativecommons.org/licenses/by/4.0/).

## 1. Introduction

The global trend of a constant increase in prices for energy resources requires an assessment of the effectiveness of the technical state of technological processes and technical systems [1]. Evaluation of the effectiveness of the technical state of technological processes and systems will make it possible to choose ways and develop algorithms for their optimization [2]. Optimization paths will reduce both mechanical and electrical losses. This fact, in turn, will affect the reduction of energy consumption of technical systems during the execution of technological processes.

On the other hand, stability [3,4] and reliability [5,6] are also topical issues when considering the efficiency of the operation of technical systems. When evaluating the reliability, it is necessary to establish the influence of the reliability of each element on the

Symmetry **2022**, 14, 1305 2 of 34

reliability of the technical system as a whole and have enough necessary information to predict the period of their trouble-free operation [7]. The main element in most modern technical systems is the electric drive [8].

Squirrel-cage induction motors are widely used in various industries and transport. They are used in technological lines of heavy engineering [9,10], as traction motors on railway rolling stock [11–13], as auxiliary equipment on railway rolling stock [14,15] and in water transport [16,17]. Thus, the quality and accuracy of the execution of technological processes depend on the technical condition of induction motors. In this regard, providing timely and reliable diagnostics of the technical condition of induction motors is an urgent modern task. Taking into account the difficult operating conditions of electrical machines and the responsibility of their functions in vehicles such as ships used in water transport or the rolling stock of railways, the task of creating a system for diagnosing the state of induction motors built into the composition of the corresponding drives is an urgent task.

In studies [18,19], an analysis of the causes of failures of induction motors and statistics of the main types of failures was carried out. From the analysis carried out in these works, it follows that the largest part of the failures is due to damage to the insulation of the windings of an induction motor. Interturn short circuits in the motor stator windings occupy a large part among the other causes of insulation damage.

The study [20] provides an overview of methods for diagnosing induction motors, and the study [21] provides an overview of modern methods for diagnosing interturn short circuits in stator windings. In these works, three main methods for diagnosing interturn short circuits are distinguished: vibration, current and temperature. The implementation of the temperature method is the most economical type of diagnostics methods used, however, the results of the interturn fault diagnostics have low accuracy and information content. When carrying out bench diagnostics, diagnostic systems based on the implementation of vibrational methods showed good results in terms of accuracy. However, when carrying out bench tests, the symmetry and sinusoidality of the supply voltage system of the induction motor is taken into account, which is not always carried out with the diagnostic system built into the drive.

It is shown in [22] that the process of changing the voltage in the contact network is a non-stationary non-deterministic process, which indicates the asymmetry and non-sinusoidality of the voltage of the power supply system of traction induction motors.

Vibration systems for diagnosing the interturn short circuit of the motor windings are based on the study of the level of vibrations during the operation of an induction motor. In works [23,24], a study was made of the effect of interturn short circuits on the operating characteristics. These works show that interturn short circuits cause torque pulsation on the motor shaft, asymmetry of the systems of the stator and rotor currents, an increase in the average value of the stator current, and a decrease in efficiency and power. Torque ripples on the shaft are used as a diagnostic parameter. In the same works, it is shown that with the same degree of damage to the stator windings, the level of pulsations during the operation of the electric motor with a load is much less than in the idle mode, which makes it difficult to identify the presence of an interturn short circuit during operation. During bench tests, diagnostics in the idle mode do not cause great difficulties, but when diagnosing an induction motor as part of a drive during its operation, this mode cannot be implemented, since the motor is under load all the time. It follows from this that the systems of vibration diagnostics in diagnosing an induction motor operating as part of a drive are less effective than in bench tests.

The asymmetry and non-sinusoidality of the voltages of the power supply system of an induction motor is the dominant factor that reduces the efficiency of diagnostic systems for a running induction motor. In [25], it is shown that the asymmetry of the power supply system of an induction motor has the same effect on its performance as the interturn short circuit. When using vibration diagnostic systems in conditions of the asymmetry and non-sinusoidality of the electric motor supply voltage system, the question of the causes of vibrations remains open.

Symmetry **2022**, 14, 1305 3 of 34

Current methods based on the measurement of phase currents [26] and the study of changes in stator currents in different phases [27] also do not allow researchers to accurately determine the reasons for the manifestation of the asymmetry of the stator current system.

The analysis of the reasons for the occurrence of asymmetry in the systems of stator currents of an induction motor is devoted to the works [28–30], in which it is proposed to determine the presence of an interturn short circuit in the stator windings of an induction motor using the Park vector. These works show that with a symmetrical system of supply voltages and the absence of an interturn circuit of the stator windings, the Park vector hodograph describes a regular circle. In the presence of an interturn short circuit, the Park vector hodograph is extended along one of the axes and takes the form of an ellipse, but these works did not investigate the effect of asymmetric voltage on the shape of the Park vector hodograph.

The solution to this issue is considered in the study [31], where the authors showed the effect of an asymmetric supply voltage system in the absence of an interturn circuit of the stator windings of an induction motor on the shape of the Park vector hodograph. It states that the asymmetry of the supply voltage system also leads to the formation of an ellipse of the Park vector hodograph, and this ellipse has an inclination relative to one of the axes.

Despite the obviously correct approach to diagnosing the presence of an interturn short circuit in the stator windings of an induction motor [28–30] and determining the effect of the asymmetry of the supply voltage system on the shape of the Park vector hodograph [31], a number of issues remain unexplored. The main issues to be considered and researched include: the separation of the influence of interturn short circuit and asymmetry of the electric motor supply voltage system from the shape of the Park vector hodograph and the determination of the degree of damage to the stator windings of the electric motor.

Thus, the development of an algorithm for separating the effect of the interturn short circuit of the stator windings and the asymmetry of the supply voltage system on the characteristics of an induction motor, as well as determining the degree of damage to its windings, is an urgent task for creating a diagnostic embedded system.

The aim of this research was to develop an algorithm for determining the degree of damage to the windings of the stator phases of an induction motor as a result of the occurrence of an interturn circuit in symmetrical and asymmetric supply voltage systems.

To accomplish the aim, the following was done:

- 1. The Park vector hodograph has been constructed under the condition that the supply voltage system is symmetrical for a different number of turns on one of the stator phases, the number of which was determined by taking into account the degree of damage to the winding (the number of closed turns). According to the hodograph diagrams of the Park vector, the values of the amplitudes of the stator phase currents and the angles of the phase shift between the current and voltage in each stator phase have been calculated. The determination of the amplitudes of the stator phase currents and the angles of the phase shift between the current and voltage have been carried out according to the time diagrams of the stator currents, after which the results have been compared;
- 2. The Park vector hodograph has been constructed under the condition of a fixed degree of damage to one of the phases of the stator winding and various values of deviations from the nominal phase supply voltage of one of the phases of the electric motor. According to the hodograph diagrams of the Park vector, the values of the amplitudes of the stator phase currents and the angles of the phase shift between the current and voltage in each stator phase have been calculated. The determination of the amplitudes of the phase currents of the stator and the angles of the phase shift between the current and voltage in each phase of the stator has been carried out according to the time diagrams of the stator currents, after which the results have been compared;

Symmetry **2022**, *14*, 1305 4 of 34

3. The Park vector hodograph has been constructed under the condition of a fixed deviation from the nominal value of the phase supply voltage of one of the phases of the electric motor and a different number of turns of the winding of one of the stator phases, taking into account various degrees of interturn short circuit. According to the hodograph diagrams of the Park vector, the values of the amplitudes of the stator phase currents and the phase shift angles between the current and voltage in each stator phase have been calculated. The determination of the amplitudes and angles of the phase shift has been carried out according to the time diagrams of the stator currents, after which the results have been compared;

- 4. The values of the amplitudes of the phase currents of the stator and the angles of the phase shift between current and voltage, obtained in Paragraphs 2 and 3, have been recalculated for the case of symmetry of the supply voltage system of the induction motor. Comparison of the received results with the results received in Point 1 has been carried out;
- An algorithm for determining the number of damaged turns of the stator winding of an induction motor has been proposed.

The advantage of the proposed method is the relative simplicity of its implementation. For its implementation, only the values of the stator phase currents are needed. In modern drive systems with vector control or direct torque control of an induction motor, current sensors are already present. In addition, the proposed method makes it possible to separate the impact of the performance of an induction motor from the unbalance of the voltage system and the unbalance of the stator windings. To do this, the authors proposed an algorithm for recalculating the projections of the hodograph vector of the Park of stator currents from an orthogonal–elliptical basis to an orthogonal–circular one. In addition, the recalculation algorithm proposed by the authors will make it possible to determine the presence or absence of an interturn short circuit in the motor stator windings and to determine the degree of damage to the stator winding.

This work can be used to build a diagnostic system for an induction motor operating as part of a drive under conditions of asymmetry of the supply voltage system.

## 2. Materials and Methods

The studies were carried out for a squirrel-cage induction motor for a simulation model made in the MATLab software environment, the principles of which are given in [32], and the implementation is in [33]. The choice of the model is due to the establishment of the adequacy of its operation both for asymmetric modes of the stator windings as a result of damage, and for the asymmetry of the supply voltage system.

Asymmetric modes of stator windings were implemented in the model based on the methodology given in [34]. On the basis of works [35–37], the simulation of the Park transform block was performed. The simulation model of an induction motor [33] was supplemented with a Park transformation block.

Under the condition of a fixed degree of damage to one of the phases of the stator winding and different values of deviation from the nominal phase supply voltage of one of the phases of the electric motor, time diagrams of the stator currents and the Park vector hodograph were obtained. According to the hodograph diagrams of the Park vector, the values of the amplitudes of the stator phase currents and the phase shift angles between the current and voltage in each stator phase were calculated. The calculations were carried out according to the method for determining the parameters of a signal presented in an orthogonal–circular basis [38–40]. The comparison of results was made for the deviation of the amplitudes of the phase currents of the stator and the angles of the phase shift between current and voltage in each phase of the stator from the nominal values.

Under the condition of a fixed deviation from the nominal value of the phase voltage of one of the phases of the electric motor and a different number of turns on one of the stator phases, corresponding to a different degree of damage to the winding, time diagrams of the stator currents and the Park vector hodograph were obtained. According to the hodograph

Symmetry **2022**, *14*, *1305* 5 of 34

diagrams of the Park vector, the values of the amplitudes of the stator phase currents and the phase shift angles between the current and voltage in each stator phase were calculated. The calculations were carried out according to the method for determining the parameters of a signal presented in an orthogonal–elliptical basis [38–40]. The comparison of results was made for the deviation of the amplitudes of the phase currents of the stator and the angles of the phase shift between the current and voltage in each phase of the stator from the nominal values.

The values of the amplitudes of the stator phase currents and the angles of the phase shift between current and voltage in each stator phase, obtained for different values of the deviation from the nominal value of the phase supply voltage of one of the phases of the electric motor, were recalculated for the case of the symmetry of the supply voltage system of the induction motor. The recalculation was carried out according to the method of transition from the orthogonal–elliptic basis to the orthogonal–circular basis of the signal representation [41–43]. The obtained results were compared with the results obtained for the condition of a fixed degree of damage to one of the phases of the stator winding and different values of deviation from the nominal value of the phase supply voltage of one of the phases of the electric motor. The comparison of results was made for the deviation of the amplitudes of the phase currents of the stator and the angles of the phase shift between the current and voltage in each phase of the stator from the nominal values.

Based on the research results, an algorithm for determining the number of damaged turns of the stator winding of an induction motor (degree of damage) was proposed. The algorithm is based on the use of the fact that the increments of the amplitudes of the stator phase currents and the phase shift angles between the current and voltage in each phase of the stator in the event of an interturn short circuit, in comparison with the nominal mode, are linear.

The object of the research is a squirrel-cage induction motor of the AIR132M4 series with a power of 11.0 kW. The technical characteristics of the AIR132M4 electric motor are given in Table 1 [23].

<b>Table 1.</b> Parameters of AIR132M4 se	eries squirrel-cage induction motor.
---	--------------------------------------

Indicators	Value
Power P, kW	11.0
Effective value of the phase voltage U <sub>nom</sub> , V	311.0
Effective value of stator current I <sub>snom</sub> , A	31.0
Rated supply voltage frequency f, Hz	50.0
Rated speed n <sub>r</sub> , rpm	1450
Number of phases n, items	3
Number of pole pairs pp, items	2
Power factor $\cos_{\varphi}$ , r. u.	0.847
Efficiency η,%	88.1
Stator winding phase active resistance $r_s$ , $\Omega$	0.5
Active resistance of the rotor winding reduced to the stator winding $r'_r$ , $\Omega$	0.36
Stator winding leakage inductance $L_{\sigma s}$ , Hn	0.001783
Rotor winding leakage inductance reduced to the stator winding, $L'_{\sigma r}$ , Hn	0.002986
Total inductance of the magnetizing circuit $L_{\mu}$ , Hn	0.07266
Number of phase turns of the stator winding w <sub>s</sub> , things	96
Number of rotor bars $Z_r$ , things	64
Stator winding length l <sub>s</sub> , m	0.163
Air gap length $l_{\beta}$ , m	0.128
Stator radius r <sub>s</sub> , m	0.255
Rotor radius $r_r$ , $m$	0.253

Symmetry **2022**, *14*, 1305 6 of 34

The values of the remaining parameters required for the organization of asymmetric regimes were obtained automatically using a simulation model [33].

## 3. Determination of the Degree of Damage to the Stator Windings during Interturn Short Circuit

3.1. Determination of the Amplitude of the Stator Phase Currents and the Angles of the Phase Shift between Current and Voltage in Each Stator Phase with the Symmetry of the Supply Voltage System for a Different Number of Turns on One of the Stator Phases

In a real induction machine, phase currents and voltages are described in three-phase ABC coordinates. The transition from three-phase coordinates to rotating two-phase coordinates dq is called the Park transformation, with the d coordinate directed along the stator phase A voltage.

When diagnosing malfunctions of an induction motor using the Park vector on a plane with coordinates dq, the Park vector hodograph was constructed. With a serviceable induction machine, the Park vector hodograph describes a regular circle, and in the presence of various types of faults, an ellipse [28–30]. This is explained by the fact that only when the system of stator windings of an asynchronous motor is balanced, the condition  $I_d \sin(\omega t) = I_q \sin(\omega t + \pi/2)$  is fulfilled. In this case, the hodograph of the Park vector will describe a circle. With an asymmetric stator winding system,  $I_d \sin(\omega t) \neq I_q \sin(\omega t + \pi/2)$ , then the hodograph of the Park vector will describe an ellipse.

The hodograph of the Park vector in the presence of faults in an induction machine is shown in Figure 1.

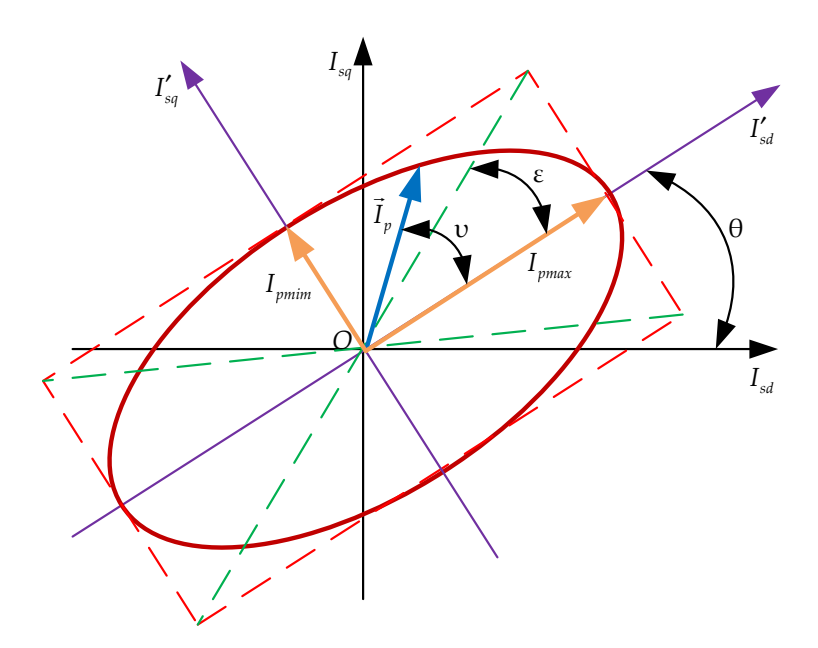


Figure 1. Park vector hodograph in the presence of faults in an induction machine.

The following designations are adopted in Figure 1:

 $\theta$ —the orientation angle of the Park vector (ellipse): the angle between the  $OI_{sd}$  axis and the main semi-axis of the ellipse);

 $\varepsilon$ —the ellipticity angle: the angle between the main semi-axis of the ellipse and the diagonal of the rectangle closest to it;

 $\upsilon$ —the angle between the main semi-axis of the ellipse and the instantaneous position of the Park vector  $\overrightarrow{I_P}$ ;

I<sub>pmin</sub>,—the values of the Park vector when it coincides with the q axis;

I<sub>pmax</sub>—the values of the Park vector when it coincides with the d axis.

Symmetry **2022**, *14*, 1305 7 of 34

The transition from ABC coordinates to dq coordinates is carried out using the formulas [35–37]:

$$\begin{cases} I_{d} = I_{A} \cdot \cos(\omega \cdot t + \phi) - \frac{1}{\sqrt{3}} \cdot (I_{B} - I_{C}) \cdot \sin(\omega \cdot t + \phi), \\ I_{q} = I_{A} \cdot \sin(\omega \cdot t + \phi) + \frac{1}{\sqrt{3}} \cdot (I_{B} - I_{C}) \cdot \cos(\omega \cdot t + \phi), \end{cases}$$
(1)

where  $I_A$ ,  $I_B$ ,  $I_C$ —the value of the phase currents of the induction motor, presented in ABC coordinates;

 $\phi$ —the phase angle of the projection of the rotating vector onto the direction of the principal semi-axis of the ellipse.

Full phase of the space vector of the stator current [35–37]:

$$\varphi(t) = \omega \cdot t + \varphi, \tag{2}$$

where  $\omega$ —the angular frequency of rotation of the coordinate plane. When choosing the rotation frequency of the coordinate plane, the following considerations were taken into account. For this problem, it is necessary to express the projections of the Park vector on both axes of the coordinate plane as a function of the angular frequency of the stator phase currents. Therefore, the angular frequency of rotation of the coordinate plane was taken to be equal to zero.

The total phase of the Park vector in some (not constant during one oscillation period) scale determines the angle  $\nu(t)$  between the main semi-axis of the ellipse and the instantaneous position of the Park vector  $\overrightarrow{I_p}$ . The angles  $\varphi(t)$  and  $\nu(t)$  are not equal in magnitude, since the Park vector rotates at different speeds during one period. Only at those times when the Park vector  $\overrightarrow{I_p}$  coincides with the semi-axes of the ellipse does the equality  $\varphi = \nu$  take place. At other times, the value of the angle  $\nu$  is found from the relationship [35–37]:

$$tgv(t) = tg\varepsilon \cdot tg\varphi(t), \tag{3}$$

so

$$\upsilon(t) \ = \ arctg[tg\epsilon \cdot tg\phi(t)] + \frac{\pi}{2} \cdot sign\{ sin \, \epsilon \cdot sin \, \phi(t) \} \cdot [1 - sign\{ cos \, \epsilon \cdot cos \, \phi(t) \}], \ \ (4)$$

where sign[a] is «sign a», so

$$sign[a] = \begin{cases} 1 \text{ at } a > 0, \\ -1 \text{ at } a < 0. \end{cases}$$
 (5)

In order to determine the phase of the spatial current vector on the diagram (Figure 1), in addition to the direction of the main semi-axis of the ellipse and the direction of the field vector, the instantaneous position of the Park vector  $\overrightarrow{I_p}$  at time t=0 is shown. Then, the angle between the Park vector  $(\overrightarrow{I_p}$  and the main semi-axis will approximately determine the phase  $\phi$  of the space vector of the stator current. Positive values of  $\phi$  are plotted in the direction of field rotation.

In the following, the angle  $\upsilon$  is called the phase of the Park vector, and the angle  $\phi$  is called the angle of the space vector of the stator current.

For research, the original simulation model of an induction motor [33] was supplemented with "Block for determining the coordinates of the Park vector" (Figure 2).

To set asymmetric power modes for an induction motor, the following changes were made to the original simulation model. In the original simulation model, the electrical part is made on the elements of the Specialized Power System library. To carry out the planned studies, the phase voltages of the stator of an induction electric motor are made in the form of a sinusoidal voltage generator of the Simulink library. The voltage of one of the phases (in this case, phase A) is multiplied by the coefficient  $k_U$ , which sets the asymmetric

Symmetry **2022**, 14, 1305 8 of 34

mode of the power system. To match the signal levels of different libraries, the signals from the generator outputs are fed to controlled voltage sources. After that, the stator supply voltages are applied to the corresponding terminals of the stator winding of the induction electric motor. The values of the controlled signals are fed into the Workspace, where, after processing, they are displayed on the corresponding graphs.

When conducting research, the change in the amplitude of phase currents during transient processes in an induction motor was taken into account, which leads to a change in the shape of the Park vector hodograph. For this purpose, starting diagrams of stator currents (Figure 3), torque (Figure 4) and motor shaft speed (Figure 5) were obtained in the simulation model.

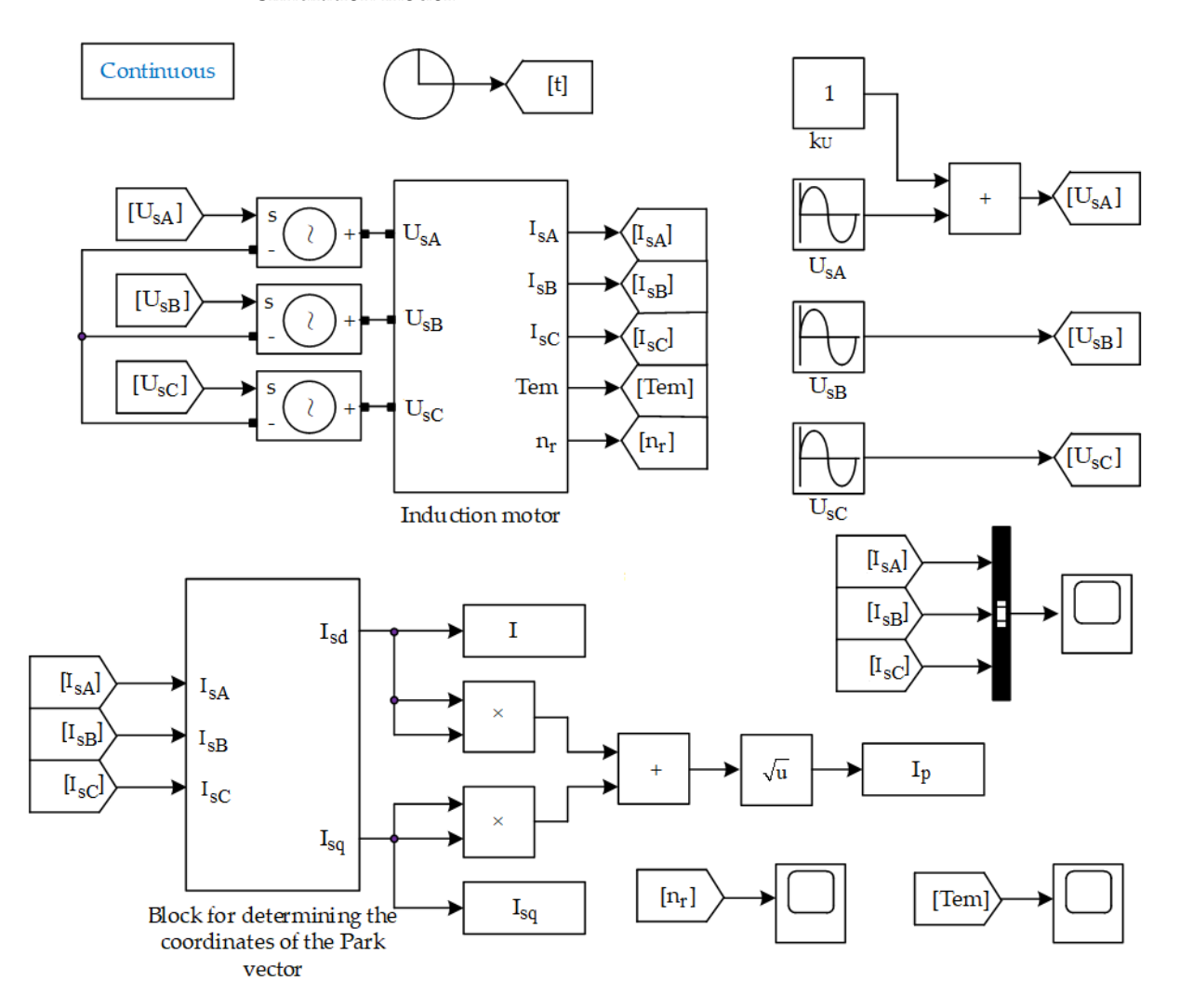


**Figure 2.** Simulation model of an induction motor with a block for calculating the coordinates of the Park vector, made in the MATLab software environment.

According to the starting diagrams, the time of the transient process was determined, which amounted to  $0.36\,\mathrm{s}$ .

To construct the hodograph of the Park vector, a time interval was adopted corresponding to two periods of the supply voltage of the stator of the induction motor, i.e., the studies were carried out in the time interval from 0.36 s to 0.4 s.

Symmetry **2022**, 14, 1305 9 of 34

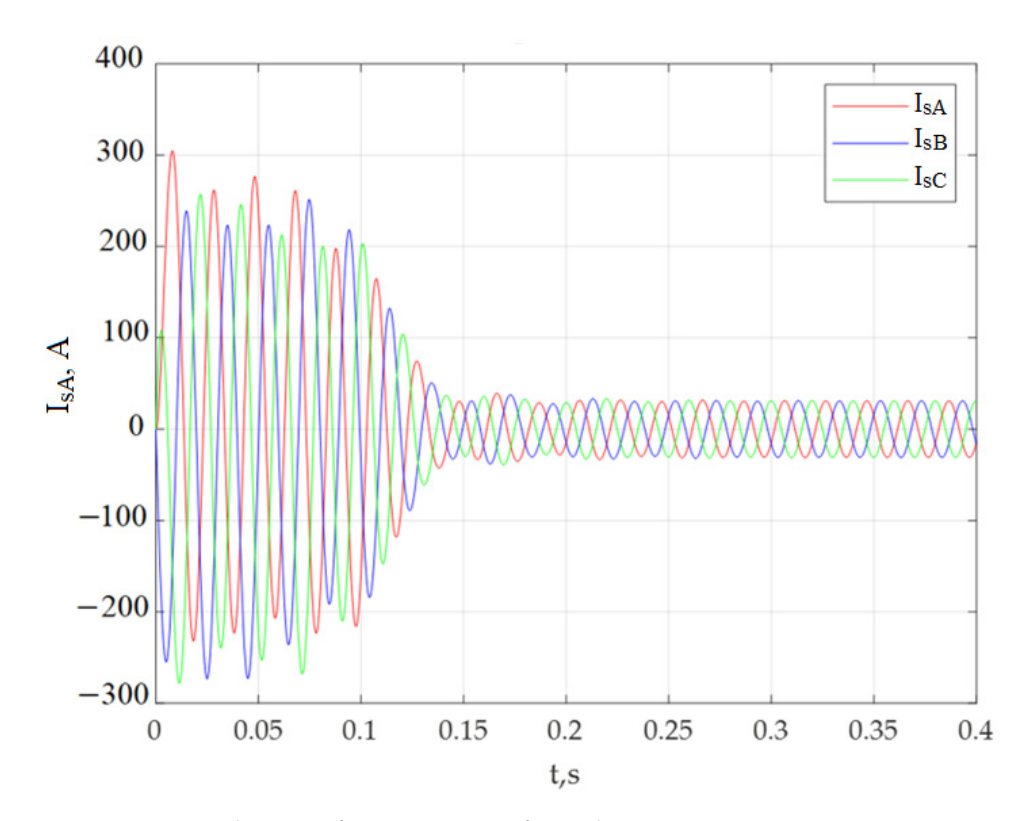


Figure 3. Starting diagram of stator currents of an induction motor.

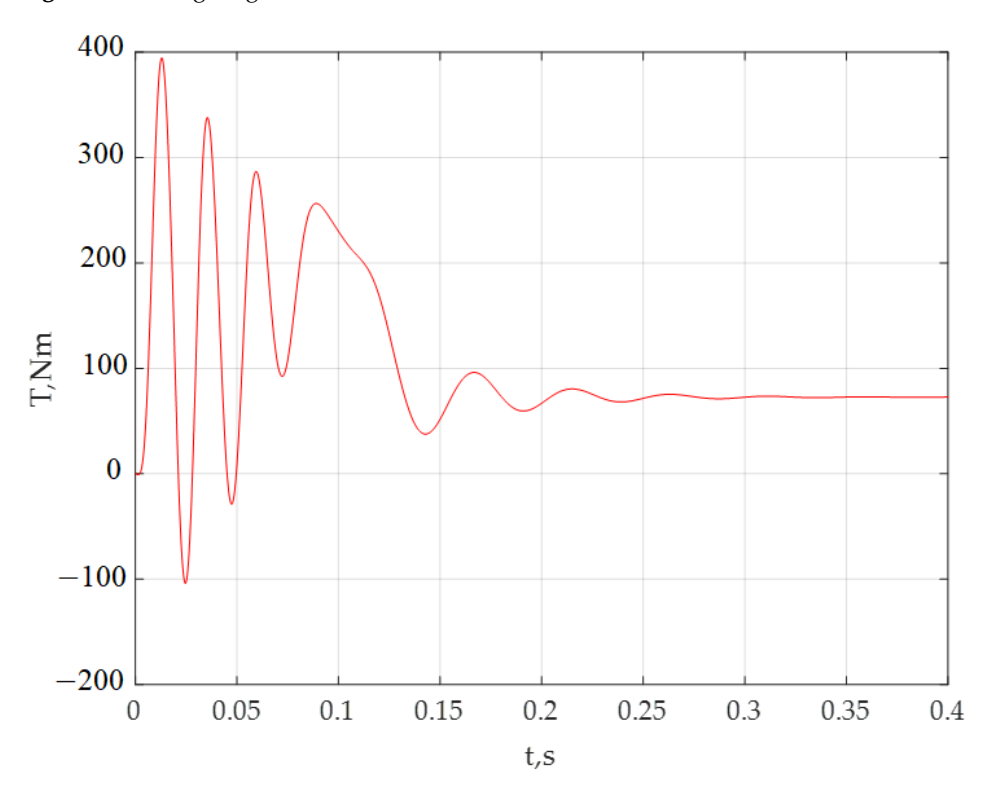


Figure 4. Starting diagram of induction motor torque Start.

Symmetry **2022**, 14, 1305 10 of 34

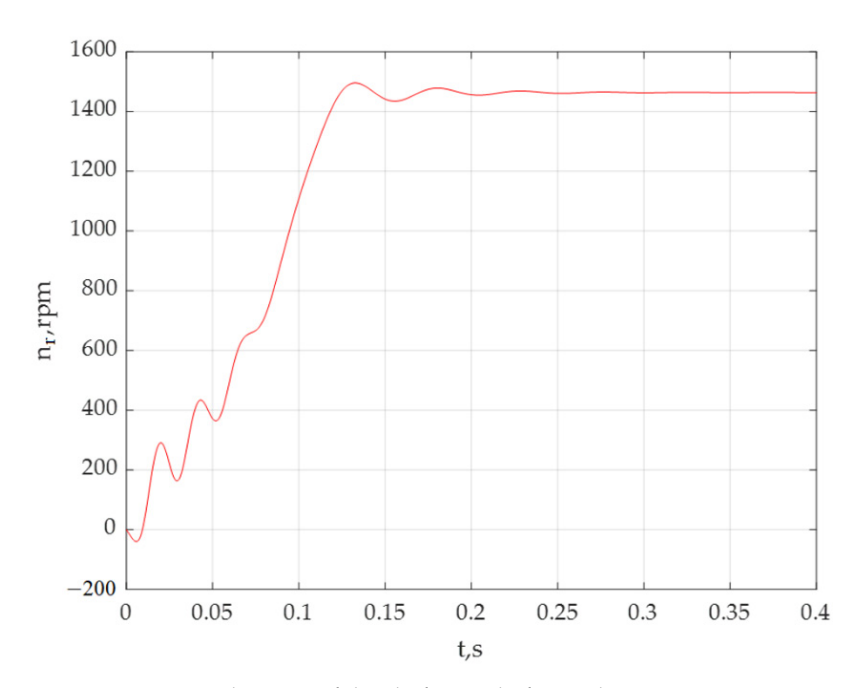
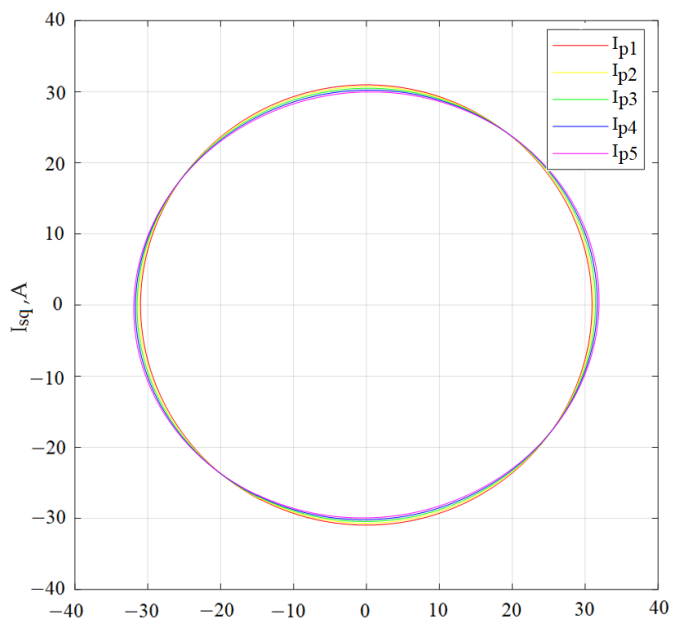


Figure 5. Starting diagram of the shaft speed of an induction motor.

The first experiment consisted of constructing the Park vector hodograph with a symmetrical power supply system for the following number of turns of the stator winding of phase A of an induction electric motor:  $w_{sA1} = 96$ ,  $w_{sA2} = 91$ ,  $w_{sA3} = 86$ ,  $w_{sA4} = 81$ ,  $w_{sA5} = 76$ , the number of which corresponds to the number of remaining undamaged turns after an interturn short circuit of varying degrees with undamaged turns of the windings of phases B and C ( $w_{sB} = 96$ ,  $w_{sC} = 96$  (see Table 1)).

For the above modes of operation, plots of the Park vector hodographs are plotted (Figure 6).



**Figure 6.** Park vector hodographs for a symmetrical power supply system of an induction motor:  $I_{p1}$ —at  $w_{sA1} = 96$ ;  $I_{p2}$ —at  $w_{sA2} = 91$ ;  $I_{p3}$ —at  $w_{sA3} = 86$ ;  $I_{p4}$ —at  $w_{sA4} = 81$ ;  $I_{p5}$ —at  $w_{sA5} = 76$  turns of the stator winding of phase A and the initial number of turns in phases B and C:  $w_{sB} = 96$ ,  $w_{sC} = 96$ .

Figure 6 defines the values of currents  $I_{sd}$  at  $I_{sq}$  = 0 and  $I_{sq}$  at I  $I_{sd}$  = 0. The results are listed in Table 2.

**Table 2.** Deviations of the amplitude and phase displacements of the stator phase currents during interturn short circuit in phase A of the stator winding.

	Number of Working Turns of the Stator w <sub>sA</sub>					
Parameter of the Park Vector	$w_{sA1} = 96$	$w_{sA2} = 91$	$w_{sA3} = 86$	$w_{sA4} = 81$	$\mathbf{w_{sA5}} = 76$	
Current value $I_{sd0}$ , at $I_{sq} = 0$ , A	30.946	31.183	31.398	31.66	31.854	
Current value $I_{sq0}$ , at $I_{sd} = 0$ , A	30.946	30.685	30.418	30.192	29.897	
Instantaneous value of the phase A stator current I <sub>sA</sub> , A	30.942	31.191	31.398	31.66	31.9	
Phase A stator current increment $\Delta I_{sA}$ , A	0	0.228	0.456	0.718	0.958	
Instantaneous value of the phase A stator current determined from the I <sub>sA</sub> diagram, A	30.946	31.183	31.398	31.659	31.853	
Phase A stator current increment determined from the diagram $\Delta I_{sAm}$ , A	0	0.237	0.452	0.713	0.903	
Error in phase A stator current increment, $\delta_{\Delta IsA}$ , %	0	3.95	0.88	0.69	5.74	
Instantaneous value of the phase B stator current I <sub>sB</sub> , A	30.942	30.788	30.634	30.48	30.326	
Phase B stator current increment $\Delta I_{sB}$ , A	0	-0.154	-0.308	-0.462	-0.616	
Instantaneous value of the phase B stator current of determined from the I <sub>sB</sub> diagram, A	30.946	30.791	30.627	30.507	30.318	
Phase B stator current increment determined from the diagram $\Delta_{IsBm}$ , A	0	-0.155	-0.319	-0.439	-0.628	
Error in determining the phase B stator current increment $\delta_{\Delta IsB}$ , %	0	0.65	3.58	5.63	2.45	
Instantaneous value of the phase C stator current I <sub>sC</sub> , A	30.942	30.808	30.674	30.54	30.406	
Phase C stator current increment $\Delta I_{sC}$	0	-0.134	-0.268	-0.402	-0.536	
Instantaneous value of the phase C stator current, determined from the I <sub>sCm</sub> diagram, A	30.946	30.81	30.667	30.567	30.401	
Phase C stator current increment determined from the diagram $\Delta I_{sCm}$ , A	0	-0.136	-0.279	-0.379	-0.545	
Error in determining the i of the phase C stator current increment, $\delta \Delta I_{sC}$ , %	0	1.49	4.1	5.72	1.23	
The phase shift angle of the phase A stator current determined on the model, $\phi I_{sAm}$ , deg.	31.32	30.921	30.522	30.123	29.724	
Displacement of the phase shift angle of phase A stator current $\Delta \phi I_{sA}$ , deg.	0	-0.399	-0.798	-1.197	-1.596	
The phase shift angle of phase A stator current determined on the model, $\phi I_{sAm}$ , deg.	31.32	30.912	30.519	30.125	29.731	
The displacement of the phase shift angle of the phase A current determined on the model $\Delta \phi I_{sAm}$ , deg.	0	-0.408	-0.801	-1.195	-1.589	
The error in determining the displacement of the phase shift angle of the phase current A, $\delta\Delta\phi_{IsA}$ , %	0	2.26	0.36	0.17	0.44	
The phase shift angle of phase B stator current $\phi I_{sB}$ , deg.	31.32	31.342	31.364	31.386	31.408	
Stator phase B current phase shift $\Delta \phi I_{sB}$ , deg.	0	0.022	0.044	0.066	0.088	
The phase shift angle of the phase B stator current determined on the model, $\phi I_{\text{sBm}}$ , deg.	31.32	31.341	31.363	31.384	31.406	
Displacement of the phase shift angle of phase B stator current determined on the model, $\Delta \phi I_{sBm}$ , deg.	0	0.021	0.043	0.064	0.086	
Error in determining the displacement of the phase shift angle of the phase current B, $\delta\Delta\phi_{IsB}$ , %	0	4.45	2.27	3.03	2.27	
Phase shift angle of the phase C stator current $\phi I_{sC}$ , deg.	31.32	31.342	31.364	31.386	31.408	

Table 2. Cont.

Parameter of the Park Vector	Number of Working Turns of the Stator w <sub>sA</sub>					
Parameter of the Park Vector	$w_{sA1} = 96$	$\mathbf{w_{sA2}} = 91$	$\mathbf{w_{sA3}} = 86$	$\mathbf{w_{sA4}} = 81$	$\mathbf{w_{sA5}} = 76$	
Phase shift angle of phase C current $\Delta \phi I_{sC}$ , deg.	0	0.022	0.044	0.066	0.088	
The phase angle of the phase C stator current determined on the model, $\phi I_{sCm}$ , deg.	31.32	31.341	31.363	31.384	31.406	
Displacement of the phase shift angle of the phase C stator current determined on the model, $\Delta \phi I_{sCm}$ , deg.	0	0.021	0.043	0.064	0.086	
Error in determining the displacement of the phase shift angle of the current C, $\delta\Delta\phi I_{sC}$ , %	0	4.45	2.27	3.03	2.27	
Ellipticity angle $\varepsilon$ , deg.	45.0	44.539	44.092	43.64	43.185	
Ellipse tilt angle $\theta$ , deg.	0	0	0	0	0	

In the simulation model, the values of the amplitudes and phases of the stator phase currents were determined. The results are listed in Table 2.

The analysis of the results given in Table 2 shows that the values of the current  $I_{sq0}$  for all modes are less than the values of the current  $I_{sd0}$  of the corresponding modes. This means that the ellipticity angle will be less than the value of  $\pi/4$  rad. In addition, the tilt angle of the ellipse is zero. This means that the family of Park vector hodographs (Figure 6) is represented in an orthogonal–circular basis.

The calculation of the ellipticity angle for an orthogonal–circular basis was carried out according to the formula [35–37]:

$$\varepsilon = \arctan \frac{I_{pmin}}{I_{pmax}}.$$
 (6)

For the Park vector, represented in the orthogonal–circular basis  $I_{pmax} = I_{sd0}$ ,  $I_{pmin} = I_{sd0}$ , a circle is formed. In this case, the circle is a partial case of an ellipse. For this case, it can be argued that the ellipticity angle for an orthogonal–circular basis  $\varepsilon$  and the ellipticity angle for an orthogonal–elliptic basis  $\gamma$  are equal, i.e.,  $\varepsilon = \gamma$ .

The phase shift angles of the stator currents were determined from the Expressions [35–37]:

$$\begin{cases} tg\phi_{IsA} = tg\gamma \cdot tg\phi_{snom}, \\ tg\phi_{IsB} = tg\gamma \cdot tg\left(\phi_{snom} - \frac{2 \cdot \pi}{3}\right), \\ tg\phi_{IsC} = tg\gamma \cdot tg\left(\phi_{snom} + \frac{2 \cdot \pi}{3}\right), \end{cases}$$
 (7)

where  $\phi_{snom}$ —the value of the phase shift angle of the stator currents with intact stator windings. Then,

$$\begin{cases} \varphi_{\text{IsAm}} = \operatorname{arctg}(tg\gamma \cdot tg\varphi_{\text{snom}}), \\ \varphi_{\text{IsBm}} = \operatorname{arctg}(tg\gamma \cdot tg(\varphi_{\text{snom}} - \frac{2 \cdot \pi}{3})), \\ \varphi_{\text{IsCm}} = \operatorname{arctg}(tg\gamma \cdot tg(\varphi_{\text{snom}} + \frac{2 \cdot \pi}{3})). \end{cases}$$
(8)

The results of calculations for the presented ratios are listed in Table 2.

The amplitudes of the stator phase currents are determined for the moment of time were obtained from the condition:

$$\omega \cdot t + \varphi_{\text{snom}} = 2 \cdot \pi. \tag{9}$$

This made it possible to neglect the component  $\omega \cdot t + \phi_{snom}$  when calculating the amplitudes of the stator phase currents.

The inverse Park transform has the form [35–37]:

$$\begin{cases} i_{sA}(t) = I_{sd0} \cdot \cos(\omega \cdot t + \phi) + I_{sq0} \cdot \sin(\omega \cdot t + \phi), \\ i_{sB}(t) = I_{sd0} \cdot \cos(\omega \cdot t + \phi - \frac{2 \cdot \pi}{3}) + I_{sq0} \cdot \sin(\omega \cdot t + \phi - \frac{2 \cdot \pi}{3}), \\ i_{sC}(t) = I_{sd0} \cdot \cos(\omega \cdot t + \phi + \frac{2 \cdot \pi}{3}) + I_{sq0} \cdot \sin(\omega \cdot t + \phi + \frac{2 \cdot \pi}{3}). \end{cases}$$
 (10)

When converting the components of a three-phase fixed coordinate system into components of an arbitrarily moving orthogonal coordinate system, the Park transformation is used. In the theory of a generalized electric machine, when modeling an induction motor, several systems of moving coordinates are used. In particular, this is a coordinate system oriented along the rotor field (dq coordinates), which is a coordinate system oriented according to the stator voltage (xy coordinates). In these models, the projections of currents on the corresponding axes are functions of the angular frequency of the rotation of the motor shaft. This makes it possible to take into account slip losses, saturation of the magnetic circuit, etc., in these models. Since this study uses a mathematical model in three-phase coordinates, which takes into account slip losses, saturation of the magnetic

wire, and magnetic losses, there is no need to take these factors into account again. On the other hand, among the tasks set, there was no task to establish the relationship between stator currents and the frequency of the rotation of the motor shaft. Therefore, the direct transformation of the Park was used with a frequency of rotation of the coordinates that was equal to the frequency of the supply voltage of the induction motor. Therefore, in Expression (10)  $\omega$  is the frequency of the supply voltage.

Since the coordinate system in Park transformations is oriented along the voltage of phase A, in Expression (10) one should use the phase shift angle of phase A  $\phi_A$  as the phase shift angle between the phase voltage and phase current  $\phi$ .

Taking into account Expression (9), the amplitudes of the stator phase currents were determined by the formulas

$$\begin{cases} I_{sAm} = \sqrt{\left(I_{sd0} \cdot \cos(\Delta \phi_{sIAm})\right)^{2} + \left(I_{sq0} \cdot \sin(\Delta \phi_{sIAm})\right)^{2}}, \\ I_{sBm} = \sqrt{\left(I_{sd0} \cdot \cos(\Delta \phi_{sIAm} - \frac{2 \cdot \pi}{3})\right)^{2} + \left(I_{sq0} \cdot \sin(\Delta \phi_{sIAm} - \frac{2 \cdot \pi}{3})\right)^{2}}, \\ I_{sCm} = \sqrt{\left(I_{sd0} \cdot \cos(\Delta \phi_{sIAm} + \frac{2 \cdot \pi}{3})\right)^{2} + \left(I_{sq0} \cdot \sin(\Delta \phi_{sIAm} + \frac{2 \cdot \pi}{3})\right)^{2}}. \end{cases}$$
(11)

The displacements of the phase shift angles of the phase currents were determined by the formulas:

$$\Delta \varphi_{\rm Ism} = \varphi_{\rm Ism} - \varphi_{\rm Ismnom}, \tag{12}$$

where  $\phi_{Ism}$ —the phase shift angle between the phase voltage and the phase current of the controlled phase, determined from the Park vector hodograph diagram for the case under study;

 $\phi_{Ismnom}$ —the phase shift angle between the phase voltage and the phase current of the controlled phase, determined from the Park vector hodograph diagram in the absence of an interturn short circuit.

When determining the displacements of the phase shift angles of phase currents according to the time diagrams  $\Delta\phi_{Ism}$  in Expression (12), the corresponding values of the angles, which were obtained from the time diagrams, were used. The calculation results are listed in Table 2.

The increment of the stator currents of the phases was determined by the formula

$$\Delta I_{sm} = I_{sm} - I_{smnom}, \tag{13}$$

where  $I_{sm}$ —the amplitude of the phase current of the controlled phase, determined from the hodograph diagram of the Park vector for the case under study;

 $I_{smnom}$ —the amplitude of the phase current of the controlled phase, determined from the hodograph diagram of the Park vector in the absence of an interturn short circuit.

When determining the displacements of the angles of the phase shift of the phase currents according to the time diagrams  $\Delta I_{sm}$  in Expression (13), the corresponding amplitude values obtained from the time diagrams were used. The calculation results are listed in Table 2.

We calculated of the error of displacements of the phase shift angles of the phase currents according to

$$\delta\Delta\phi_{\rm I} = \frac{|\Delta\phi_{\rm Ism} - \Delta\phi_{\rm Is}|}{\Delta\phi_{\rm Is}} \cdot 100\% \tag{14}$$

and increments of stator phase current

$$\delta \Delta I_{s} = \frac{|\Delta I_{sm} - \Delta I_{s}|}{\Delta \varphi_{Is}} \cdot 100\%. \tag{15}$$

The calculation results are listed in Table 2.

Symmetry **2022**, *14*, 1305 15 of 34

3.2. Determination of the Amplitude of the Stator Phase Currents and the Phase Shift Angles between Current and Voltage in Each Stator Phase for the Number of Turns on the Damaged Stator Phase with Asymmetry of the Supply Voltage System

The second experiment consisted of constructing the Park vector hodograph in the presence of 86 turns of the damaged stator phase A winding for the following values of phase A phase supply voltage:  $U_{sA1} = 311$  V,  $U_{sA2} = 308$  V,  $U_{sA3} = 305$  V,  $U_{sA4} = 302$  V,  $U_{sA5} = 299$  V at nominal values of phase voltages of phases B and C ( $U_{sB} = U_{sC} = 311$  V (Table 1)).

For the specified modes of operation, plots of the Park vector hodographs were constructed (Figure 7).

Figure 7 defines the values of the currents  $I_{sd}$  at  $I_{sq}$  = 0,  $I_{sq}$  at  $I_{sd}$  = 0, the maximum value of the Park vector  $I_{pmax}$ , the minimum value of the Park vector  $I_{pmin}$ , the value of the current  $I_{sd}$  at  $I_p$  =  $I_{pmax}$ , and the value of the current  $I_{sq}$  at  $I_p$  =  $I_{pmax}$ . The results are listed in Table 3.

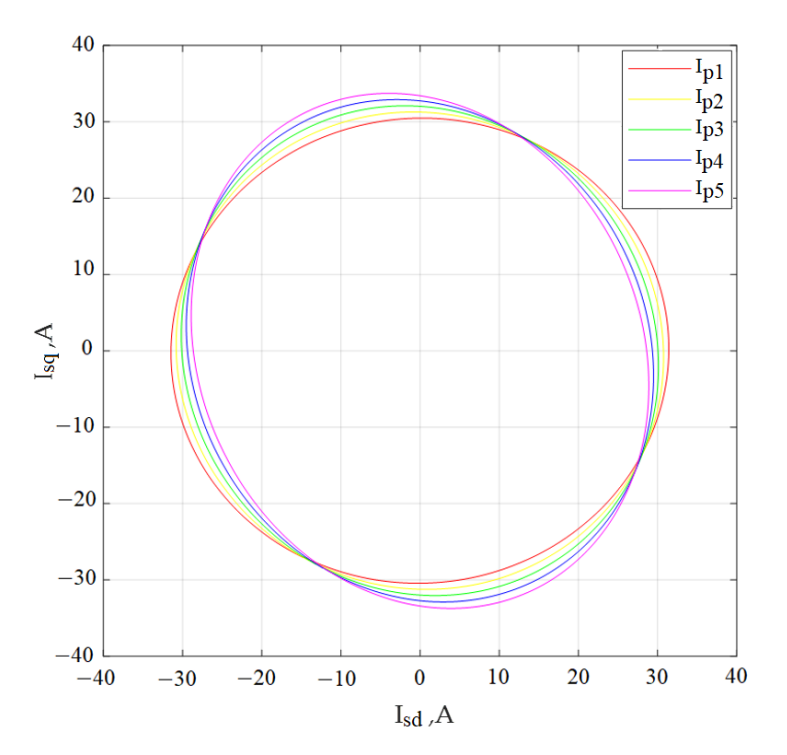


**Figure 7.** Park vector hodographs for an asymmetric power supply system of an induction motor with  $w_{sA} = 86$  turns of the stator phase A winding and 96 undamaged turns of the B and C phase windings:  $I_{p1}$ —at  $U_{sA1} = 311$  V;  $I_{p2}$ —at  $U_{sA2} = 308$  V;  $I_{p3}$ —at  $U_{sA3} = 305$  V;  $I_{p4}$ —at  $U_{sA4} = 302$  V;  $I_{p5}$ —at  $U_{sA5} = 299$  V and nominal values of phase voltages of phases B and C ( $U_{sB} = U_{sC} = 311$  V).

In the simulation model, the values of the amplitudes and phases of the stator phase currents were determined. The results are listed in Table 3.

The calculation of the ellipticity angle for an orthogonal–circular basis was performed according to (6).

The calculation of the ellipticity angle for an orthogonal–elliptic basis was carried out according to the formula:

$$\gamma = \arctan \frac{I_{sq0}}{I_{sd0}}.$$
 (16)

The angle of inclination of the ellipse is determined by the formula

$$\theta = \arccos \frac{I_{sd}}{I_{pmax}} = \arcsin \frac{I_{sq}}{I_{pmax}}.$$
 (17)

**Table 3.** Deviations of the amplitude and phase displacements of the stator phase currents at  $w_{sA}$  = 86 turns of the winding of phase A and 96 turns of phases B and C with a change in the phase voltage of phase A and the rated voltages of phases B and C.

	Stator Phase Voltage U <sub>sA</sub> , V					
Parameter of the Park Vector	$U_{sA1} = 311$	$U_{sA2} = 308$	$U_{sA3} = 305$	$U_{sA4} = 302$	$U_{sA5} = 299$	
Current value $I_{sd0}$ , at $I_{sq} = 0$ , A	31.398	30.85	29.985	29.3453	28.6192	
Current value $I_{sq0}$ , at $I_{sd} = 0$ , A	30.418	31.2674	32.0223	32.7419	33.4207	
Current value $I_{sd}$ , at $I_p = I_{pmax}$ , A	31.398	15.6837	12.4823	12.088	12.0614	
Current value $I_{sq}$ , at $I_p = I_{pmax}$ , A	30.418	-27.3015	-31.9624	-31.1955	-32.2805	
The maximum value of the Park vector I <sub>pmax</sub> , A	31.398	31.4875	32.4585	33.4552	34.4603	
The minimum value of the Park vector I <sub>pmin</sub> , A	30.418	30.5226	29.6975	28.7509	28.0216	
Instantaneous value of the phase A stator current I <sub>sA</sub> , A	31.398	30.875	30.039	29.37	28.694	
Phase A stator current increment $\Delta I_{sA}$ , A	0	-0.523	-1.359	-2.028	-2.704	
Instantaneous value of the phase A stator current determined from the I <sub>sA</sub> diagram, A	31.398	30.85	29.987	29.354	28.645	
Phase A stator current increment determined from the diagram $\Delta I_{sAm}$ , A	0	-0.548	-1.411	-2.044	-2.753	
Error in determining the phase A stator current increment, $\delta \Delta I_{sA}$ , %	0	5.25	3.83	0.79	1.81	
Instantaneous value of the phase B stator current I <sub>sB</sub> , A	30.634	31.169	31.653	32.138	32.551	
Phase B stator current increment $\Delta I_{sB}$ , A	0	0.535	1.019	1.504	1.917	
Instantaneous value of the phase B stator current determined from the I <sub>sB</sub> diagram, A	30.627	31.18	31.601	32.048	32.453	
Phase B stator current increment determined from the diagram $\Delta I_{sBm}$ , A	0	0.533	0.974	1.421	1.826	
Error in determining the phase B stator current increment, $\delta\Delta I_{sB}$ , %	0	0.38	4.42	5.52	4.75	
Instantaneous value of the phase C stator current increment I <sub>sC</sub> , A	30.674	31.169	31.505	31.906	32.263	
Phase C stator current increment $\Delta I_{sC}$ , A	0	0.495	0.831	1.232	1.589	
Instantaneous value of the phase C stator current determined from the I <sub>sC</sub> diagram, A	30.667	31.164	31.528	31.933	32.301	
Phase C stator current increment determined from the diagram $\Delta I_{sCm}$ , A	0	0.497	0.861	1.266	1.634	
Error in determining the phase C stator current increment, $\delta\Delta I_{sC}$ , %	0	0.4	3.61	2.78	2.83	
The phase shift angle of the phase A stator current $\phi_A$ , deg.	30.522	31.634	32.973	34.122	35.342	
The displacement of the phase shift angle of phase A stator current $\Delta \phi I_{sA}$ , deg.	0	1.112	2.451	3.6	4.82	
The phase shift angle of the phase A stator current determined on the model, $\phi I_{sAm}$ , deg.	30.519	31.663	33.017	34.173	35.397	
The displacement of phase shift angle of the phase A stator current determined on the model $\Delta \phi I_{sA}$ , deg.	0	1.144	2.498	3.654	4.878	
Error in determining the displacement of the phase shift angle of the phase current A, $\delta\Delta I_{sA}$ , %	0	2.88	1.92	1.5	1.2	
The phase shift angle of phase B stator current $\phi I_{sB}$ , deg.	31.364	31.304	31.244	31.184	31.124	
Stator phase B current phase shift $\Delta \varphi I_{sB}$ , deg.	0	-0.06	-0.12	-0.18	-0.24	
The phase shift angle of the phase B stator current determined on the model, $\phi I_{sBm}$ , deg.	31.363	31.302	31.236	31.183	31.13	
The displacement of the phase shift angle of the phase B stator current determined on the model, $\Delta \phi I_{sBm}$ , deg.	0	-0.061	-0.127	-0.18	-0.233	

Table 3. Cont.

		Stator	Phase Voltage	U <sub>sA</sub> , V	
Parameter of the Park Vector	$U_{sA1} = 311$	$U_{sA2} = 308$	$U_{sA3} = 305$	$U_{sA4} = 302$	$U_{sA5} = 299$
Error in determining the displacement of the phase shift angle of the phase current B, $\delta\Delta\phi I_{sB}$ , %	0	1.67	5.83	0	2.92
The phase shift angle of the phase C stator current $\varphi I_{sC}$ , deg.	31.364	31.304	31.244	31.184	31.124
Stator phase C current phase shift $\Delta \varphi I_{sC}$ , deg.	0	-0.06	-0.12	-0.18	-0.24
The phase angle of the phase C Stator phase B current phase shift determined on the model, $\varphi I_{sCm}$ , deg.	31.363	31.302	31.236	31.183	31.13
The displacement of phase shift angle of the phase C stator current determined on the model, $\Delta \varphi I_{sCm}$ , deg.	0	-0.061	-0.127	-0.18	-0.233
Error in determining the displacement of the phase shift angle of the phase current C, $\delta\Delta\phi I_{sC}$ , %	0	1.67	5.83	0	2.92
Ellipticity angle in orthogonal–circular basis $\varepsilon$ , deg.	44.092	44.109	42.457	40.675	39.116
Ellipticity angle in orthogonal–elliptic basis $\gamma$ , deg.	44.092	45.479	46.822	48.131	49.426
Ellipse tilt angle $\theta$ , deg.	0	-60.124	-68.668	-68.819	-69.512

The phase shift angles of the stator currents were determined from (8). The calculation results are listed in Table 2.

The amplitudes of the stator phase currents were determined by (11).

The displacements of the phase shift angles of the phase currents were determined by (12).

When determining the displacements of the phase shift angles of the phase currents according to the time diagrams  $\Delta\phi_{Ism}$  in Expression (12), the corresponding values of the angles obtained from the time diagrams were used. The calculation results are listed in Table 3.

The increments of the stator currents of the phases were calculated according to (13). When determining the displacements of the phase shift angles of the phase currents according to the time diagrams  $\Delta I_{sm}$  in Expression (13), the corresponding amplitude

according to the time diagrams  $\Delta I_{sm}$  in Expression (13), the corresponding amplitude values obtained from the time diagrams were used. The calculation results are listed in Table 3.

The errors in the displacements of the phase shift angles of the phase currents were calculated by the Formula (14), the increments of the stator current of the phases were calculated by the Formula (15). The calculation results are listed in Table 3.

3.3. Determination of the Amplitude of the Stator Phase Currents and the Angles of the Phase Shift between Current and Voltage in Each Stator Phase at a Fixed Degree of Asymmetry of the Supply Voltage System for a Different Number of Turns on One of the Stator Phases

The third experiment consisted of constructing the Park vector hodograph at phase A voltage equal to  $U_{sA} = 305$  V at the nominal values of phase voltages of phases B and C ( $U_{sB} = U_{sC} = 311$  V) for the following number of turns of the stator winding of phase A of an induction motor:  $w_{sA1} = 96$ ,  $w_{sA2} = 91$ ,  $w_{sA3} = 86$ ,  $w_{sA4} = 81$ ,  $w_{sA5} = 76$ , the number of which corresponded to the number of remaining undamaged turns after an interturn short circuit of varying degrees with undamaged turns of the windings of phases B and C ( $w_{sB} = 96$ ,  $w_{sC} = 96$ , Table 1).

For the indicated modes of operation of the induction motor, the plots of the Park vector hodographs were constructed (Figure 8).

Figure 8 defines the values of the currents  $I_{sd}$  at  $I_{sq}$  = 0,  $I_{sq}$  at  $I_{sd}$  = 0, the maximum value of the Park vector  $I_{pmax}$ , the minimum value of the Park vector  $I_{pmin}$ , the value of the current  $I_{sd}$  at  $I_p$  =  $I_{pmax}$ , and the value of the current  $I_{sq}$  at  $I_p$  =  $I_{pmax}$ . The results are listed in Table 4.

In the simulation model, the values of the amplitudes of the phase currents of the stator and the phase shift angles between the current and voltage in each phase of the stator were determined. The results are listed in Table 4.

The calculation of the ellipticity angle for an orthogonal–circular basis was performed according to (6); the calculation of the ellipticity angle for an orthogonal–elliptical basis was performed according to (16).

In this case, the ellipse tilt angle was determined by (17), the phase shift angles of the stator currents from Expressions (8), the amplitudes of the stator phase currents by Formula (11), and the displacement of the phase shift angles of phase currents by (12). The calculation results are listed in Table 4.

When determining the displacements of the phase shift angles of the phase currents according to the time diagrams  $\Delta\phi_{Ism}$  in Expression (12), the corresponding values of the angles obtained from the time diagrams were used. The calculation results are also listed in Table 4.

The increments of the stator current of the phases were determined by (13). When determining the displacements of the phase shift angles of the phase currents from the time diagrams  $\Delta I_{sm}$  in Expression (13), the corresponding amplitude values obtained from the time diagrams were used. The calculation results are listed in Table 4.

**Table 4.** Deviations of amplitude and phase displacements of phase currents of the stator at phase voltage of phase A— $U_{sA}$  = 305 V and nominal values of phase voltages of phases B and C ( $U_{sB}$  =  $U_{sC}$  = 311 V) during an interturn short circuit in phase A of the stator winding.

	Number of Working Turns of the Stator w <sub>sA</sub>					
Parameter of the Park Vector	$w_{sA1} = 96$	$w_{sA2} = 91$	$w_{sA3} = 86$	$w_{sA4} = 81$	$w_{sA5} = 76$	
Current value $I_{sd0}$ , at $I_{sq} = 0$ , A	28.6982	29.8262	29.985	30.0266	30.5748	
Current value $I_{sq0}$ , at $I_{sd} = 0$ , A	29.3945	32.2536	32.0223	31.79	31.5465	
Current value $I_{sd}$ , at $I_p = I_{pmax}$ , A	10.5215	11.4475	12.4823	14.706	16.2856	
Current value $I_{sq}$ , at $I_p = I_{pmax}$ , A	-30.7401	-30.6181	-31.9624	-29.0098	-27.6087	
The maximum value of the Park vector I <sub>pmax</sub> , A	32.933	32.6881	32.4585	32.245	32.0541	
The minimum value of the Park vector Ipmin, A	29.291	29.4919	29.6975	29.8965	30.0804	
Instantaneous value of the phase A stator current I <sub>sA</sub> , A	28.76	30.01	30.039	30.04	30.57	
Phase A stator current increment $\Delta I_{sA}$ , A	0	1.09	1.341	1.28	1.81	
Instantaneous value of the phase A stator current determined from the I <sub>sA</sub> diagram, A	28.698	29.829	29.987	30.028	30.575	
The increment of the phase A stator current determined from the diagram $\Delta I_{sAm}$ , A	0	1.131	1.289	1.33	1.877	
Error in determining the phase A stator current increment, $\delta\Delta I_{sA}$ , %	0	3.76	3.88	3.91	3.7	
Instantaneous value of the phase B stator current I <sub>sB</sub> , A	29.25	31.686	31.653	31.446	31.35	
Phase B stator current increment $\Delta I_{sB}$ , A	0	2.436	2.403	2.196	2.1	
Instantaneous value of the phase B stator current determined from the I <sub>sB</sub> diagram, A	29.249	31.753	31.601	31.424	31.343	
Phase B stator current increment determined from the diagram $\Delta I_{sBm}$ , A	0	2.504	2.352	2.175	2.094	
Error in determining the phase B stator current increment, $\delta\Delta I_{sB}$ , %	0	2.8	2.12	0.96	0.29	
Instantaneous value of the phase C stator current increment I <sub>sC</sub> , A	29.06	31.582	31.505	31.229	31.06	
Phase C stator current increment $\Delta I_{sC}$ , A	0	2.522	2.445	2.169	2.0	
Instantaneous value of the phase C stator current determined from the I <sub>sC</sub> diagram, A	29.222	31.668	31.528	31.36	31.307	
Phase C stator current increment determined from the diagram $\Delta I_{sCm}$ , A	0	2.446	2.306	2.138	2.085	
Error in determining the phase C stator current increment, $\delta\Delta I_{sC}$ , %	0	3.01	5.69	1.43	4.25	
The phase shift angle of the phase A stator current $\varphi_A$ , deg.	31.91	33.28	32.973	32.741	32.094	
Offset of phase shift angle of stator phase A current $\Delta \phi I_{sA}$ , deg.	0	1.37	1.061	0.831	0.184	
The phase shift angle of the phase A stator current determined on the model, $\phi I_{sAm}$ , deg.	31.933	33.345	33.017	32.791	32.122	
The displacement phase shift angle of the stator phase A current determined on the model $\Delta \phi I_{sA}$ , deg.	0	1.412	1.084	0.858	0.189	
The error in determining the displacement of the phase shift angle of the phase current A, $\delta\Delta I_{sA}$ , %	0	3.07	2.17	3.25	2.72	
The phase shift angle of phase B stator current $\phi I_{sB}$ , deg.	31.299	31.233	31.244	30.258	31.278	
Stator phase B current phase shift $\Delta \phi I_{sB}$ , deg.	0	-0.066	-0.055	-0.041	-0.021	
The phase shift angle of the phase B stator current determined on the model, $\phi I_{\text{sBm}}$ , deg.	31.289	31.221	31.236	31.247	31.279	
Offset of phase shift angle of stator phase B current determined on the model, $\Delta\phi I_{sBm}$ , deg.	0	-0.068	-0.053	-0.042	-0.02	

Table 4. Cont.

	Number of Working Turns of the Stator w <sub>sA</sub>					
Parameter of the Park Vector	$w_{sA1} = 96$	$w_{sA2} = 91$	$w_{sA3} = 86$	$w_{sA4} = 81$	$\mathbf{w_{sA5}} = 76$	
Error in determining the displacement of the phase shift angle of the phase current B, $\delta\Delta\phi I_{sB}$ , %	0	3.03	3.64	2.444	4.76	
The phase shift angle of the phase C stator current $\phi I_{sC}$ , deg.	31.299	31.233	31.244	30.258	31.278	
Stator phase C current phase shift $\Delta \varphi I_{sC}$ , deg.	0	-0.066	-0.055	-0.041	-0.021	
The phase angle of the phase C Stator phase B current phase shift determined on the model, $\varphi I_{sCm}$ , deg.	31.289	31.221	31.236	31.247	31.279	
Offset of phase shift angle of stator phase C current determined on the model, $\Delta \phi I_{sCm}$ , deg.	0	-0.068	-0.053	-0.042	-0.02	
Error in determining the displacement of the phase shift angle of the phase current C, $\delta\Delta\phi I_{sC}$ , %	0	3.03	3.64	2.444	4.76	
Ellipticity angle in orthogonal–circular basis $\varepsilon$ , deg.	41.65	42.057	42.457	42.836	43.181	
Ellipticity angle in orthogonal–elliptic basis $\gamma$ , deg.	45.687	47.239	46.822	46.634	45.896	
Ellipse tilt angle $\theta$ , deg.	-71.105	-69.5	-68.668	-63.118	-59.465	

Symmetry **2022**, *14*, 1305 21 of 34

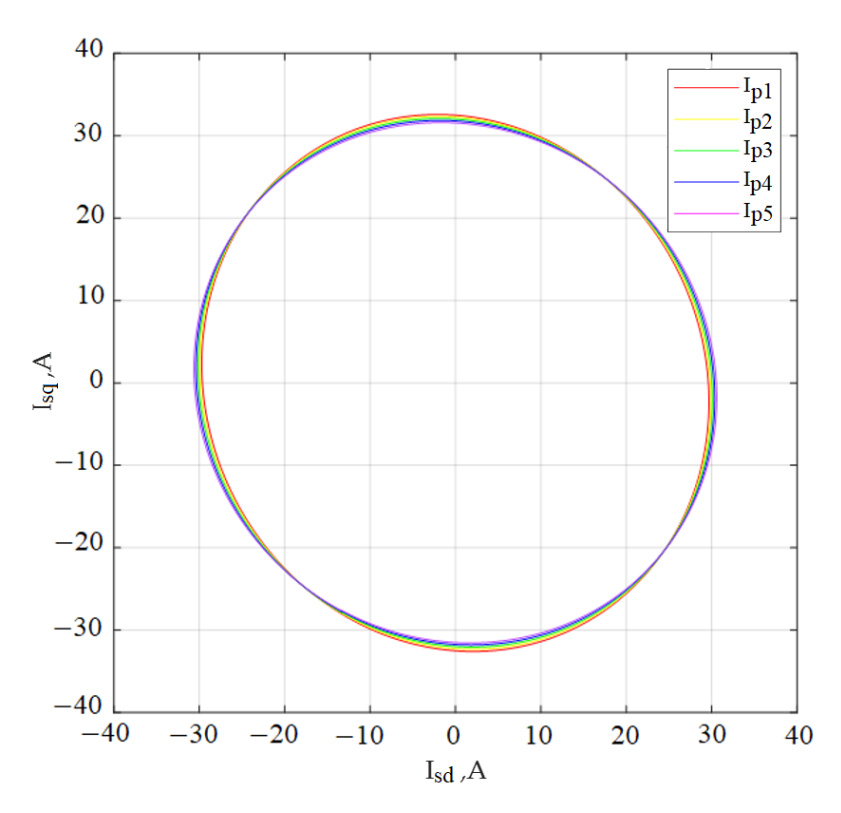


**Figure 8.** Park vector hodographs at the phase voltage of phase A— $U_{sA}$  = 305 V and the nominal values of the phase voltages of phases B and C ( $U_{sB}$  =  $U_{sC}$  = 311 V):  $I_{p1}$ —at  $w_{sA1}$  = 96;  $I_{p2}$ —at  $w_{sA2}$  = 91;  $I_{p3}$ —at  $w_{sA3}$  = 86;  $I_{p4}$ —at  $w_{sA4}$  = 81;  $I_{p5}$ —at  $w_{sA5}$  = 76 turns of the stator winding of phase A and undamaged turns of the windings of phases B and C.

The errors in the displacement of the phase shift angles of the phase currents were calculated according to (14) and the increments of the stator current of the phases were calculated according to (15). The calculation results are listed in Table 4.

3.4. Determination of the Amplitude of the Stator Phase Currents and the Phase Shift Angles between Current and Voltage in Each Stator Phase for Cases in Paragraphs 3.2 and 3.3 with a Symmetrical Supply Voltage System of an Induction Motor

In Experiments 2 (Section 3.2) and 3 (Section 3.3), the Park vector hodograph was obtained in an orthogonal-elliptic basis. The presence of asymmetry in the power supply system of an induction motor was evidenced by the angle of inclination of the Park vector hodograph relative to the OI<sub>sd</sub> axis (Figures 7 and 8 and Tables 3 and 4), the value of which is not equal to zero [31]. The analysis of the nature of the behavior of the Park vector hodograph in case of an unbalance of the power supply system is based on the analysis of the symmetrical components of the supply voltage system of an induction motor. Since the sources of phase voltages are connected by a "Y", there is no zero sequence for both balanced and unbalanced supply voltage systems. With a balanced supply voltage system, there is only a positive sequence, since the negative sequence is zero. With an unbalanced supply voltage system, the negative sequence is not equal to zero. This factor leads to the fact that with a balanced system of supply voltages, the angle of inclination of the ellipse relative to the axis Id is equal to zero, and with an unbalanced system of supply voltages, the angle of inclination of the ellipse relative to the axis Id is not equal to zero. With a balanced system of supply voltages and with a symmetrical system of stator windings, the hodograph of the Park vector describes a circle, and with an asymmetric system of stator windings, an ellipse. With an unbalanced system of supply voltages, both with a symmetrical and asymmetric system of stator windings, the hodograph of the Park vector will describe an ellipse.

When recalculating the amplitudes and phases of the phase currents obtained in the presence of asymmetry of the voltage system of the induction motor, the instantaneous values of the currents  $i'_{sd0}$  and  $i'_{sq0}$  were calculated in an orthogonal–circular basis according to the formulas [38–40]:

$$i'_{sd0} = (\cos \varepsilon_0 \cdot \cos \theta_0 - j \cdot \sin \varepsilon_0 \cdot \sin \theta_0) \cdot I_{pmax} \cdot \cos \theta + + j \cdot (\cos \varepsilon_0 \cdot \sin \theta_0 + j \cdot \sin \varepsilon_0 \cdot \cos \theta_0) \cdot I_{pmax} \cdot \sin \theta,$$
(18)

$$i'_{sq0} = \left(\cos(-\varepsilon_0) \cdot \cos\left(\theta_0 + \frac{\pi}{2}\right) - j \cdot \sin(-\varepsilon_0) \cdot \sin\left(\theta_0 + \frac{\pi}{2}\right)\right) \cdot I_{pmax} \cdot \cos\theta + + j \cdot \left(\cos(-\varepsilon_0) \cdot \sin\left(\theta_0 + \frac{\pi}{2}\right) + j \cdot \sin(-\varepsilon_0) \cdot \cos\left(\theta_0 + \frac{\pi}{2}\right)\right) \cdot I_{pmax} \cdot \sin\theta,$$
(19)

where  $\varepsilon_0$ —the ellipticity angle of the basis unit vector along the d axis in the new basis. Along the q axis, the value of this angle is  $-\varepsilon_0$ . For an orthogonally circular basis,  $\varepsilon_0 = \pi/4$ ;

 $\theta_0$ —the ellipse tilt angle of the basis vector along the d axis in the new basis. Along the q axis, the value of this angle is  $\theta_0 + \pi/2$ . For an orthogonally circular basis,  $\theta_0 = 0$ .

The amplitude values of the currents  $i^\prime_{sd0}$  and  $i^\prime_{sq0}$  were calculated using the formulas

$$\begin{cases} I'_{sd0} = \sqrt{(Re(i'_{sd0}))^2 + (Im(i'_{sd0}))^2}, \\ I'_{sq0} = \sqrt{(Re(i'_{sq0}))^2 + (Im(i'_{sq0}))^2}. \end{cases}$$
(20)

The calculation of the ellipticity angle of the Park vector for a new orthogonal–circular basis was carried out according to (6) with the substitution of the calculated values of  $I'_{sd0}$  and  $I'_{sq0}$ .

The phase shift angles of the stator currents were determined from Expressions (8) with the substitution of the calculated values of  $I'_{sd0}$  and  $I'_{sq0}$ .

The amplitudes of the stator phase currents were determined by (11) with the substitution of the calculated values of  $I'_{sd0}$  and  $I'_{sq0}$ .

The displacements of the angles of the phase shift of the phase currents were calculated by Formula (12).

When determining the displacements of the angles of the phase shift of the phase currents according to the time diagrams  $\Delta \phi I_{sm}$  in Expression (12), the corresponding values of the angles obtained from the time diagrams were used.

The increments of the stator current of the phases were determined by (13) with the substitution of the calculated values of  $I'_{sd0}$  and  $I'_{sq0}$ 

When determining the displacements of the phase shift angles of the phase currents from the time diagrams  $\Delta I_{sm}$  in Expression (13), the corresponding amplitude values obtained from the time diagrams were used.

The errors of displacements of the phase shift angles of the phase currents were calculated according to (14) and increments of the stator current of the phases were calculated according to (15).

The calculation results for Experiment 2 are shown in Table 5, for Experiment 3—in Table 6.

**Table 5.** Deviations of the amplitudes and displacements of the phase shift angles of the stator currents with 86 turns of the stator winding in phase A and intact windings of phases B and C (96 turns) and a change in the phase voltage of phase A at the rated phase voltages of phases B and C.

n (d n l v )		Stator	Phase Voltage	U <sub>sA</sub> , V	
Parameter of the Park Vector	$U_{sA1} = 311$	$U_{\rm sA2} = 308$	$U_{\rm sA3}=305$	$U_{\rm sA4} = 302$	$U_{sA5} = 299$
$I_{sd0}$ current value determined for a symmetrical supply voltage system at $I_{sq} = 0$ , A	31.398	31.398	31.398	31.398	31.398
Current value $I_{sq0}$ , determined for a symmetrical system of supply voltages, at $I_{sd} = 0$ , A	30.418	30.418	30.418	30.418	30.418
Current value $I'_{sd0}$ , recalculated for the condition that the power supply system is symmetrical at $I_{sq} = 0$ , A	31.398	31.395	31.4	31.398	31.397
The current value $I'_{sq0}$ , recalculated for the condition that the power supply system is symmetrical at $I_{sd} = 0$ , A	30.418	30.415	30.419	30.421	30.418
Instantaneous value of the phase A stator current determined for a symmetrical system of supply voltages, IsA, A	31.398	31.398	31.398	31.398	31.398
The increment of the phase A stator current determined for a symmetrical system of supply voltages, $\Delta I_{sA}$ , A	0.452	0.452	0.452	0.452	0.452
The instantaneous value of the phase A stator current recalculated for the condition that the power system is symmetrical IsA, A	31.398	31.395	31.4	31.398	31.397
Phase A stator current increment recalculated for the condition that the power supply system is symmetrical $\Delta I_{sAm}$ , A	0.452	0.449	0.454	0.452	0.451
Error in determining the phase A stator current increment, $\gamma \Delta I_{sA}$ , %	0	0.66	0.44	0	0.66
Instantaneous value of the phase B stator current, determined for a symmetrical system of supply voltages IsB, A	30.634	30.634	30.634	30.634	30.634
Phase B stator current increment determined for symmetrical supply voltage system $\Delta I_{sB}$ , A	-0.308	-0.308	-0.308	-0.308	-0.308
Instantaneous value of the phase B stator current increment, recalculated for the condition that the power system is symmetrical I <sub>sB</sub> , A	30.634	30.624	30.628	30.629	30.627
Phase B stator current increment determined from the diagram $\Delta I_{sBm}$ , A	-0.308	-0.322	-0.318	-0.317	-0.319
The error in determining the phase B stator current increment, in terms of the condition that the power supply system is symmetrical $\gamma\Delta I_{sB}$ , %	0	4.54	3.25	2.84	3.57
Instantaneous value of the phase C stator current determined for a symmetrical system of supply voltages I <sub>sC</sub> , A	30.667	30.667	30.667	30.667	30.667
Phase C stator current increment determined for a symmetrical system of supply voltages $\Delta I_{sC}$ , A	-0.279	-0.279	-0.279	-0.279	-0.279
Instantaneous value of the phase C stator current recalculated for the condition that the power system is symmetrical I <sub>sC</sub> , A	30.667	30.664	30.668	30.669	30.666
Phase C stator current increment determined from the diagram $\Delta I_{sCm}$ , A	-0.279	-0.282	-0.278	-0.277	-0.28
Error in determining the phase C stator current increment, $\gamma \Delta I_{sC}$ , %	0	1.08	0.36	0.72	0.36
The phase shift angle of the phase A stator current determined for a symmetrical system of supply voltages $\phi_A$ , deg.	30.522	30.522	30.522	30.522	30.522
Displacement of the phase shift angle of phase A current determined for a symmetrical system of stator supply voltages $\Delta \phi I_{sA}$ , deg.	-0.798	-0.798	-0.798	-0.798	-0.798
The phase shift angle of the of phase A stator current, in terms of the condition that the power supply system is symmetrical, $\phi A_m$ , deg.	30.522	30.519	30.518	30.522	30.52
The displacement of the phase shift angle of the phase A stator current, in terms of the condition that the power supply system is symmetrical $\Delta \phi I_{sA}$ , deg.	0	-0.801	-0.802	-0.798	-0.8
Error in determining the displacement of the phase shift angle of the phase current, $\gamma \Delta I_{sA}$ , %	0	0.38	0.501	0	0.25
The phase shift angle of the phase B stator current determined for a symmetrical system of supply voltages $\varphi_B$ , deg.	31.364	31.364	31.364	31.364	31.364
The displacement of the phase shift angle of the stator phase B determined for a symmetrical supply voltage system $\Delta \phi I_{sB}$ , deg.	0.044	0.044	0.044	0.044	0.044
The phase shift angle of the phase B stator current, in terms of the condition that the power supply system is symmetrical, $\phi B_m$ , deg.	31.364	31.363	31.363	31.362	31.362
The displacement of the phase shift angle of the current of phase B of the stator, in terms of the condition that the power supply system is symmetrical, $\Delta \phi I_{sB}$ , deg.	0.044	0.043	0.044	0.044	0.044
Error in determining the displacement of the phase shift angle of the phase current B, $\gamma\Delta I_{sB}$ , %	0	2.33	0	0	0
The phase angle of phase C stator current determined for a symmetrical system of supply voltages $\varphi$ C, deg.	31.364	31.364	31.364	31.364	31.364
The displacement of the phase shift angle of the phase C stator current determined for a symmetrical system of supply voltages $\Delta \phi I_{sC}$ , deg.	0.044	0.044	0.044	0.044	0.044

Symmetry **2022**, 14, 1305 24 of 34

Table 5. Cont.

Parameter of the Park Vector	Stator Phase Voltage $U_{sA}$ , $V$					
Parameter of the Park Vector	$U_{sA1} = 311$	$U_{\rm sA2} = 308$	$U_{sA3} = 305$	$U_{sA4} = 302$	$U_{sA5} = 299$	
The phase shift angle of the phase C stator current, in terms of the condition that the power system is symmetrical, $\phi C_m$ , deg.	31.364	31.363	31.363	31.362	31.362	
The displacement of the phase shift angle of the phase C stator current, in terms of the condition that the power supply system is symmetrical, $\Delta \phi I_{sC}$ , deg.	0.044	0.043	0.044	0.044	0.044	
Error in determining the displacement of the phase shift angle of the phase current C, $\gamma \Delta I_{sC}$ , %	0	2.33	0	0	0	
The ellipticity angle in the new orthogonal–circular basis $\varepsilon$ , deg.	44.092	44.092	44.091	44.095	44.093	

**Table 6.** Deviations of the amplitudes and displacements of the phase shift angles of the stator currents at phase voltage  $U_{sA} = 305 \text{ V}$  of phase A at nominal values of the phase voltages of phases B and C ( $U_{sB} = U_{sC} = 311 \text{ V}$ ) and interturn short circuit in phase A of the stator of various degrees of damage.

Parameter of the Park Vector	N	umber of Wo	rking Turns o	f the Stator w	sA
Parameter of the Park Vector	$w_{sA1} = 96$	$w_{sA2} = 91$	$w_{sA3} = 86$	f the Stator $w_{sA}$ $w_{sA4} = 81$ $31.66$ $30.192$ $31.661$ $30.196$ $31.66$ $0.718$ $31.66$ $0.718$ $0$ $30.48$ $-0.462$ $30.51$ $-0.435$ $5.84$ $30.54$ $-0.402$ $30.57$ $-0.376$ $6.47$ $30.123$	$w_{sA5} = 76$
$I_{\rm sd0}$ current value determined for a symmetrical supply voltage system at $I_{\rm sq}=0$ , A	30.946	31.183	31.398	31.66	31.854
Current value $I_{sq0}$ , determined for a symmetrical system of supply voltages, at $I_{sd} = 0$ , A	30.946	30.685	30.418	30.192	29.897
Current value $I'_{sd0}$ , recalculated for the condition that the power supply system is symmetrical at $I_{sq} = 0$ , A	30.947	31.183	31.4	31.661	31.853
The current value $I'_{sq0}$ , recalculated for the condition that the power supply system is symmetrical at $\hat{I}_{sd} = 0$ , A	30.945	30.681	30.419	30.196	29.893
Instantaneous value of the phase A stator current determined for a symmetrical system of supply voltages, I <sub>sA</sub> , A	30.942	31.191	31.398	31.66	31.9
The increment of the phase A stator current determined for a symmetrical system of supply voltages, $\Delta I_{sA}$ , A	0	0.228	0.456	0.718	0.958
The instantaneous value of the phase A stator current recalculated for the condition that the power system is symmetrical I <sub>sA</sub> , A	30.947	31.183	31.4	31.66	31.852
Phase A stator current increment recalculated for the condition that the power supply system is symmetrical $\Delta I_{sAm}$ , A	0	0.236	0.453	0.718	0.905
Error in determining the phase A stator current increment, $\gamma\Delta I_{sA}$ , %	0	3.51	0.66	0	5.53
Instantaneous value of the phase B stator current, determined for a symmetrical system of supply voltages I <sub>sB</sub> , A	30.942	30.788	30.634	30.48	30.326
Phase B stator current increment determined for symmetrical supply voltage system $\Delta I_{sB}$ , A	0	-0.154	-0.308	-0.462	-0.616
Instantaneous value of the phase B stator current increment, recalculated for the condition that the power system is symmetrical IsB, A	30.945	30.788	30.628	30.51	30.315
Phase B stator current increment determined from the diagram $\Delta I_{sBm}$ , A	0	-0.157	-0.317	-0.435	-0.63
The error in determining the phase B stator current increment, in terms of the condition that the power supply system is symmetrical $\gamma\Delta I_{sB}$ , %	0	1.95	2.92	5.84	2.27
Instantaneous value of the phase C stator current determined for a symmetrical system of supply voltages I <sub>sC</sub> , A	30.942	30.808	30.674	30.54	30.406
Phase C stator current increment determined for a symmetrical system of supply voltages $\Delta I_{sC}$ , A	0	-0.134	-0.268	-0.402	-0.536
Instantaneous value of the phase C stator current recalculated for the condition that the power system is symmetrical I <sub>sC</sub> , A	30.946	30.807	30.668	30.57	30.397
Phase C stator current increment determined from the diagram $\Delta I_{sCm}$ , A	0	-0.139	-0.278	-0.376	-0.549
Error in determining the phase C stator current increment, $\gamma \Delta I_{sC}$ , %	0	3.73	3.73	6.47	2.43
The phase shift angle of the phase A stator current determined for a symmetrical system of supply voltages $\phi_A$ , deg.	31.32	30.921	30.522	30.123	29.724

Table 6. Cont.

	N	umber of Wo	rking Turns o	-1.197 -1.5 30.128 29.7 -1.19 -1. 0.36 0.3 31.386 31.4 0.066 0.08 31.384 31.4 0.064 0.08 3.03 1.1 31.386 31.4 0.066 0.08 31.384 31.4 0.066 0.08 31.384 31.4 0.066 31.384 31.4	sA
Parameter of the Park Vector	$w_{sA1} = 96$	$w_{sA2} = 91$	$w_{sA3} = 86$		$\mathbf{w_{sA5}} = 76$
Displacement of the phase shift angle of phase A current determined for a symmetrical system of stator supply voltages $\Delta \phi I_{sA}$ , deg.	0	-0.399	-0.798	-1.197	-1.596
The phase shift angle of the of phase A stator current, in terms of the condition that the power supply system is symmetrical, $\varphi A_m$ , deg.	31.318	30.909	30.518	30.128	29.728
The displacement of the phase shift angle of the phase A stator current, in terms of the condition that the power supply system is symmetrical $\Delta \varphi I_{sA}$ , deg.	0	-0.409	-0.8	-1.19	-1.59
Error in determining the displacement of the phase shift angle of the phase current, $\gamma \Delta I_{sA}$ , %	0	2.51	0.25	0.36	0.38
The phase shift angle of the phase B stator current determined for a symmetrical system of supply voltages $\varphi_B$ , deg.	31.32	31.342	31.364	31.386	31.408
The displacement of the phase shift angle of the stator phase B determined for a symmetrical supply voltage system $\Delta \varphi I_{sB}$ , deg.	0	0.022	0.044	0.066	0.088
The phase shift angle of the phase B stator current, in terms of the condition that the power supply system is symmetrical, $\phi B_m$ , deg.	31.32	31.342	31.363	31.384	31.407
The displacement of the phase shift angle of the current of phase B of the stator, in terms of the condition that the power supply system is symmetrical, $\Delta \varphi I_{sB}$ , deg.	0	0.022	0.043	0.064	0.087
Error in determining the displacement of the phase shift angle of the phase current B, $\gamma \Delta I_{sB}$ , %	0	0	2.27	3.03	1.14
The phase angle of phase C stator current determined for a symmetrical system of supply voltages $\varphi$ C, deg.	31.32	31.342	31.364	31.386	31.408
The displacement of the phase shift angle of the phase C stator current determined for a symmetrical system of supply voltages $\Delta \varphi I_{sC}$ , deg.	0	0.022	0.044	0.066	0.088
The phase shift angle of the phase C stator current, in terms of the condition that the power system is symmetrical, $\varphi C_m$ , deg.	31.32	31.342	31.363	31.384	31.407
The displacement of the phase shift angle of the phase C stator current, in terms of the condition that the power supply system is symmetrical, $\Delta \phi I_{sC}$ , deg.	0	0.022	0.043	0.064	0.087
Error in determining the displacement of the phase shift angle of the phase current C, $\gamma \Delta I_{sC}$ , %	0	0	2.27	3.03	1.14
The ellipticity angle in the new orthogonal–circular basis $\epsilon$ , deg.	44.998	44.535	44.091	43.643	43.182

Symmetry **2022**, 14, 1305 26 of 34

3.5. Algorithm for Determining the Degree of Damage to the Stator Winding with an Asymmetric System of Electric Motor Supply Voltages

For further research, according to the results of Table 2, the dependences of the deviations of the amplitudes of the phase currents as a function of the number of damaged turns of the stator windings (Figure 9) and the displacements of the angles of the phase shift of the stator currents, as a function of the number of damaged turns of the stator windings (Figure 10) were plotted. The construction of dependences was performed for the values determined from the time diagrams.

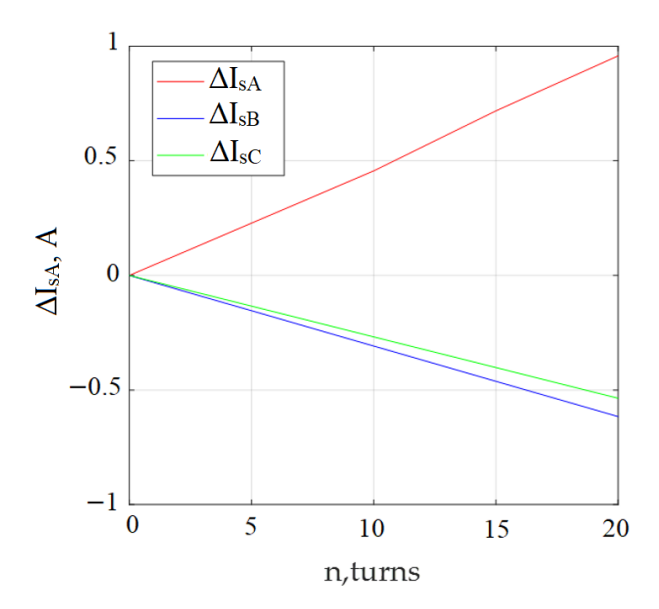


Figure 9. Deviations of phase current amplitudes from the number of damaged turns of the stator windings:  $\Delta I_{sA}$ —phase A phase current deviation;  $\Delta I_{sB}$ —phase current deviation of phase B;  $\Delta I_{sc}$ —phase current deviation of phase C.

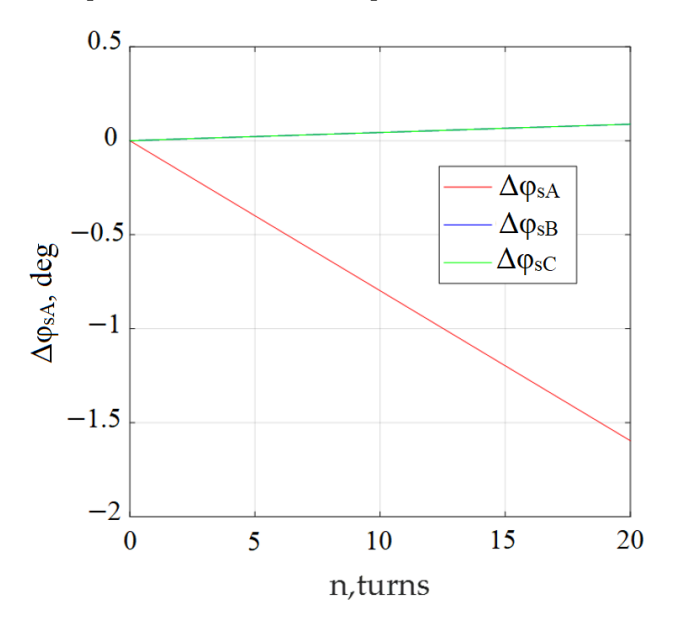


Figure 10. Displacements in the phase shift angles of the stator currents on the number of damaged turns of the stator windings:  $\Delta\phi_{sA}$ —displacement in the phase shift angle of the phase A currents;  $\Delta\phi_{sB}$ —displacement in the phase shift angle of the phase B currents;  $\Delta\phi_{sC}$ —displacement in the phase shift angle of the phase C currents.

Symmetry **2022**, 14, 1305 27 of 34

From Figures 9 and 10 it follows that the dependences of the amplitude deviations as a function of the number of damaged turns of the stator windings and the dependences of the displacements of the phase shift angles of the stator currents, as a function of the number of damaged turns of the stator windings, are linear. In this regard, the equation for determining the amplitude deviations as a function of the number of damaged turns of the stator windings can be represented as

$$\Delta I_s = k_{Is} \cdot n, \tag{21}$$

where k<sub>Is</sub>—the angular coefficient of the stator current increment, A/turn;

n—the number of damaged turns, a turn.

The angular coefficient of the increment of the stator current was calculated by the formula

$$k_{Is} = \frac{I_{si} - I_{snom}}{n_i}, \tag{22}$$

where  $I_{si}$ —the instantaneous value of the phase current of the stator of the controlled phase, for the current experiment, A;

I<sub>snom</sub>—instantaneous rated value of the stator phase current, A;

n<sub>i</sub>—the number of damaged turns for the current experiment, a turn.

According to Table 2, the angular coefficients of the increment of the stator current were calculated. For the damaged phase A, the value of the angular coefficient of the stator current increment is  $k_{\rm IsA}$  = 0.0479 A/turn; for phase B  $k_{\rm IsB}$  = -0.0308 A/turn; for phase C  $k_{\rm IsC}$  = -0.0268 A/turn.

Similarly, an expression is presented for determining the displacements of the phase shift angles of the stator currents.

$$\Delta \varphi_{Is} = k_{\omega Is} \cdot n, \tag{23}$$

where  $k_{\omega Is}$ —slope of the stator current phase shift angle, deg/turn.

The angular displacement coefficient of the phase shift angle of the stator current was calculated by the formula

$$k_{\phi Is} = \frac{\phi_{Isi} - \phi_{Isnom}}{n_i}, \tag{24}$$

where  $\phi_{Isi}$ —the value of the phase shift angle of the stator current of the controlled phase for the current experiment, deg;

 $\varphi_{Isnom}$ —the nominal value of the stator current phase shift angle, deg;

n<sub>i</sub>—the number of damaged turns for the current experiment, a turn.

According to Table 2, the slope coefficients of the stator current phase shift angle were calculated for each phase of the stator winding. For phase A, which has an interturn short circuit that leads to a decrease in the number of working turns, the value of the angular coefficient of displacement of the phase shift angle of the stator current is  $k_{\phi IsA} = -0.0798 \ deg/turn$ ; for intact phase  $B-k_{\phi IsB} = 0.0044 \ deg/turn$ ; for intact phase  $C-k_{\phi IsC} = 0.0044 \ deg/turn$ .

The damaged phase was selected by the largest value of the modulus of the slope of the stator current increment and the largest value of the slope of the phase shift angle.

Based on the studies carried out, the algorithm for determining the number of damaged turns of the stator winding in case of an interturn short circuit on one of their stator phases is as follows:

1. According to the hodograph diagram of the Park vector, the following is determined: the value of the current  $I_{sd0}$  at  $I_{sq} = 0$ , the value of the current  $I_{sq0}$ , at  $I_{sd} = 0$ , the maximum value of the Park vector  $I_{pmax}$ , the minimum value of the Park vector  $I_{pmin}$ , the value of the current  $I_{sd}$ , at  $I_p = I_{pmax}$ ;

Symmetry 2022, 14, 1305 28 of 34

> 2. Calculate the ellipticity angle for an orthogonal–circular basis using Formula (6), calculation of the ellipticity angle for an orthogonal-elliptical basis by Formula (16) and calculation of the ellipse tilt angle by Formula (17).

- If the ellipse tilt angle is not equal to zero, which indicates a supply asymmetry, the values of the currents  $I'_{sd0}$  and  $I'_{sq0}$  are determined and recalculated for an orthogonalcircular basis according to Formulas (18)-(20);
- 4. The calculation of the amplitudes and phase shift angles of the stator currents is carried out according to the Formulas (8), (10) and (11);
- 5. According to the obtained amplitudes and phase shift angles of the stator currents for each phase, the number of damaged turns is calculated using the formulas:

$$n = \frac{I_s - I_{snom}}{k_{Is}},$$

$$n = \frac{\phi_{Is} - \phi_{Isnom}}{k_{\phi Is}}.$$
(25)

$$n = \frac{\phi_{Is} - \phi_{Isnom}}{k_{\varphi Is}}.$$
 (26)

The results are rounded up to the nearest higher whole number. Among the results obtained, the largest integer is selected and a conclusion is made about the number of damaged turns.

An example of the practical use of research results.

When analyzing the performance of the proposed method, the authors used the results of the experiments presented above. As an example, the results for the unbalance condition of the power supply system ( $U_{sa} = 305 \text{ V}$ ,  $U_{sb} = U_{sc} = 311 \text{ V}$ ) and the unbalance of the stator windings ( $w_{sa} = 81$ ,  $w_{sb} = w_{sc} = 96$  undamaged turns) were used. The following was determined: current value  $I_{sd0}$ , at  $I_{sq} = 0$ , A, equal to 30.0266 A, current value  $I_{sq0}$ , at  $I_{sd} = 0$ , A, equal to 31.79, the maximum value of the Park vector  $I_{pmax}$ , 32.245 A, current value  $I_{sd}$ , at  $I_p = I_{pmax}$ , equal to 14.706 A, current value  $I_{sq}$ , at  $I_p = I_{pmax}$ , -29.0098 A (Table 4).

According to Formula (17), the ellipse tilt angle was calculated, the value of which was -63.118 deg. Since the angle of inclination of the ellipse was not equal to zero, it was concluded that the supply voltage system is unbalanced.

The projections of the ellipse from the orthogonal–elliptic basis to the orthogonal–circular basis were recalculated using Formulas (18) and (19). The amplitude values of current projections in an orthogonally circular basis were obtained using Formula (20). The results obtained were:  $I'_{sd} = 31.66 \text{ A}$ ,  $I'_{sq} = 30.192 \text{ A}$ . Using Formula (6), the angle of ellipticity was determined, the value of which was 43.64 deg. The conclusion was made about the unbalance of the stator windings.

According to Formula (8), the angles of the stator currents were calculated, the values of which were:  $\varphi_{IsAm} = 30.125$  deg.,  $\varphi_{IsBm} = 31.384$  deg.,  $\varphi_{IsCm} = 31.384$  deg. According to Formula (11), the values of the amplitudes of the stator phase currents were determined, the values of which were:  $I_{sAm} = 31.659 \text{ A.}$ ,  $I_{sBm} = 30.507 \text{ A.}$ ,  $I_{sCm} = 30.567 \text{ A.}$ 

According to Formula (12), the displacements of the phase shift angles of the phase currents were determined, the values of which were:  $\Delta \phi_{IsAm} = -1.195 \text{ deg.}$ ,  $\Delta \phi_{IsBm} = 0.064 \text{ deg.}$ ,  $\Delta \phi_{IsCm} = 0.066$  deg. According to Formula (13), the displacements of the amplitudes of the stator phase currents were determined, the values of which were:  $\Delta I_{sAm} = 0.713$  A.,  $\Delta I_{sBm} = -0.439 \text{ A.}, \Delta I_{sCm} = -0.402 \text{ A.}$ 

According to Formula (25), the number of damaged windings was calculated through the displacement of the amplitudes of the phase currents of each phase. The calculation gave the following results: the number of damaged turns, calculated through the displacement of the amplitude of the phase current of phase A  $n_{IA} = 14.885$ ; through the displacement of the phase current of phase  $B-n_{IB} = 14.253$ ; through the displacement of the phase current of phase C—n<sub>IB</sub> = 15. According to Formula (26), the number of damaged windings was calculated through the displacement of the phase shift angles of the phase currents. The calculation gave the following results: the number of damaged turns, calculated through the displacement of the phase shift angles of the phase current of phase A  $\varphi_{IA}$  = 14.945; through the shift of phase angles of the phase current of phase B— $n_{\phi B}$  = 14.545; through

Symmetry **2022**, 14, 1305 29 of 34

the shift of the phase angles of the phase current of the phase C— $n_{\phi B}$  = 14.545. The highest value was 15 damaged turns. It was concluded that 15 turns were damaged in the induction motor. This result corresponds to the setting conditions of the experiment.

## 4. Discussion

In this paper, the Park vector hodograph method was chosen as a method for diagnosing damage to the stator winding of an induction motor.

This was due to the following factors:

- When building a diagnostic system for an induction motor operating as part of a drive, the Park vector hodograph method has a higher accuracy than temperature methods;
- 2. When building a diagnostic system for an induction motor operating as part of a drive, the supply voltage system may be asymmetrical. The asymmetry of the supply voltage system, in its effect on performance, has the same negative effect as the interturn short circuit of the stator windings, with similar processes occurring. First of all, the asymmetry of the rotating stator field leads to the occurrence of torque ripples on the motor shaft. Existing methods of vibration diagnostics do not allow for determining the causes of these pulsations. As shown in the paper, the Park vector hodograph method allows the solving of problems of this type.

Three experiments were carried out in the work:

- with a symmetrical system of supply voltages and varying degrees of interturn short circuit of the stator winding of one of the phases, which were implemented by taking into account the reduced number of working turns of the winding phase with a step of five turns (Figure 6, Table 2);
- with a fixed number of turns of the damaged stator winding of one phase and various degrees of asymmetry of the supply voltage system, which were implemented by adopting a series of interphase voltage values with a step of 3 V (Figure 7, Table 3);
- with a fixed degree of asymmetry of the supply voltage system and various degrees of damage to the stator winding of one of the phases (Figure 8, Table 4).

The analysis of the results of the first experiment showed that the indicator of the presence of an interturn short circuit is the ellipticity angle of the Park vector hodograph. In the absence of damaged turns, the hodograph of the Park vector describes a circle and the ellipticity angle for this case is  $\pi/4$ . In the presence of an interturn closure, the hodograph of the Park vector describes an ellipse (Figure 6), while the ellipticity angle decreases. Analysis of the results of Table 2 showed that with an increase in the number of damaged turns, the ellipticity angle decreases.

The analysis of the results of the second experiment showed that the indicator of the presence of asymmetry in the system of supply voltages is the angle of inclination of the ellipse (Figure 7). With an increase in asymmetry, the angle of inclination of the ellipse increases (Figure 7, Table 3). The analysis of the nature of the behavior of the Park vector hodograph in case of an unbalance of the power supply system was based on the analysis of the symmetrical components of the supply voltage system of an induction motor. When the supply voltage system is balanced, the zero sequence is equal to zero, and the positive and negative sequences are equal to each other. This factor leads to the fact that when the power system is unbalanced, the angle of inclination of the ellipse relative to the Id axis is equal to zero, and when the stator winding system is balanced, the Park vector hodograph describes a circle. When the supply voltage system is unbalanced, the zero sequence is not equal to zero; the reverse and positive sequences are not equal to each other. This factor leads to the fact that both in the case of balance and unbalance of the stator winding system, the Park vector hodograph has the shape of an ellipse, the angle of inclination of which is not equal to zero.

Based on the data obtained from the diagrams of the Park vector hodographs, the amplitudes and phases of the stator currents of all phases of the induction motor were

Symmetry **2022**, 14, 1305 30 of 34

calculated (Tables 2–4). Based on the results obtained, the deviations of the amplitudes and displacements of the phase shift angles of the stator currents were calculated. According to the time diagrams of the stator currents, the amplitudes and phases of the stator currents of all phases of the induction motor were also determined, according to which the deviations of the amplitudes and displacements of the phase shift angles of the stator currents were calculated. The comparison of the results obtained from the time diagrams and using the Park vector hodograph was performed. Based on the data obtained, the errors in determining the deviations of the amplitudes and displacements of the phase shift angles of the stator currents, obtained using the Park vector hodograph, were calculated. The calculation errors did not exceed 6%.

For Experiments 2 and 3, in order to eliminate the negative effect on the phase currents and the angles of the phase currents of the stator of unbalance in the supply, the data obtained were recalculated in a new orthogonal–circular basis (Tables 5 and 6). Errors in comparing the obtained values of amplitude deviations and displacements of the phase shift angles of the stator currents with the results for a symmetrical power supply system (Table 2) did not exceed 6%.

The proposed algorithm for determining the degree of damage to the stator windings makes it possible to determine the damaged phase and the number of damaged turns, including in the presence of asymmetry in the power system.

However, when using the research results, it must be taken into account that during the experiments, assumptions were made that only one of the phases of the stator windings of an induction motor had damage. It is assumed that all other engine components were intact. The paper also considered the case of when the deviation from the nominal value of the phase voltage occurs on one phase.

These factors impose certain restrictions on the use of the developed algorithm. To take into account these factors, it is necessary to conduct a cycle of additional studies in the operating conditions of the electric motor.

The comparison of the results of diagnosing an interturn short circuit in the stator windings of an induction motor with the results given in the works of other authors gave the following results. The authors in the works [44,45] proposed definitions of methods for determining the interturn short circuit at the early stages of defect development using a method based on the analysis of the forward and reverse sequences of the stator current system. Despite the high accuracy of the results obtained, these works do not consider the possibility of using the proposed methods in the case of an unbalance of the supply voltage system of an induction motor. The work [46] proposes a hybrid analytical approach that combines the genetic approach and firing simulation. In the work [46], as well as in the works [44,45], a high accuracy of the results was obtained. But, as in the works [44,45], the possibility of the proposed method under conditions of unbalance of the supply voltage system of an induction motor was not considered. The work [47] was devoted to the determination of interturn short circuit in the windings of an induction motor with an unbalance in the supply voltage system of an induction motor. The implementation of the algorithm proposed in [47] requires a large amount of initial data. In addition, none of the listed works provide an algorithm for determining the number of damaged turns.

The advantage of the proposed method is the relative simplicity of its implementation. For its implementation, only the values of the stator phase currents are needed. In modern drive systems with vector control or direct torque control of an induction motor, current sensors are already present. In addition, the proposed method allows us to separate the impact on the performance of an induction motor from the unbalance of the voltage system and the unbalance of the stator windings. To do this, the authors proposed an algorithm for recalculating the projections of the park hodograph vector of the stator currents from an orthogonal–elliptical basis to an orthogonal–circular one. In addition, the recalculation algorithm proposed by the authors will make it possible to determine the presence or absence of an interturn short circuit in the motor stator windings and determine the degree of damage to the stator winding.

Symmetry **2022**, 14, 1305 31 of 34

However, in the process of working on this article, the authors encountered objective difficulties associated with the impossibility of conducting a full-scale experiment and thereby obtaining reliable experimental data. This is due to the fact that induction motors operating as part of the drive are constantly in the operating mode during their operation. The organization of an interturn circuit in the motor windings can lead to its failure and the disruption of the technological process.

The disadvantages of the work include:

- The interturn short circuit on one of the stator phases was investigated. The mode of occurrence of an interturn short circuit at the same time during several phases remained unexplored;
- 2. The influence of the non-sinusoidal nature of the supply voltage system was not taken into account.

Further research may include:

- 1. Development of a diagnostic system for an induction motor as part of a drive;
- Development of a diagnostic system for a drive with an induction motor powered by a three-phase autonomous voltage inverter.

#### 5. Conclusions

As a result of a complex of studies of the diagnostics of interturn short circuit in the phase of the stator winding of an induction electric motor, under the condition of an asymmetric power source, the Park vector hodograph method was proposed. Based on the research results, an algorithm for implementing the considered diagnostic method in the electric drive system was developed to identify the damaged phase and the number of short-circuited turns. Obtaining complete information about the type and degree of damage is relevant when predicting the residual life of an electric motor during its operation. In the course of the research, the following types of work were carried out:

1. The Park vector hodograph was constructed under the condition that the supply voltage system is symmetrical for a different number of damaged turns on one of the stator phases. According to the hodograph diagrams of the Park vector, the values of the amplitudes of the stator phase currents and the phase shift angles between the current and voltage in each stator phase were calculated. Values of the deviations of amplitudes and shifts of angles of phase shift of stator currents were calculated for the various cases of winding phase damage.

The amplitudes of the phase currents of the stator and the phase shift angles between the current and voltage in each phase of the stator were determined from the time diagrams of the stator currents. The values of displacement of amplitudes and displacement of the phase shift angles of stator currents were calculated. The error in calculating the values of displacements of amplitudes and displacements of the phase shift angles of the stator currents did not exceed 6%;

2. The Park vector hodograph was constructed under the condition of a fixed degree of damage to one of the phases of the stator winding and different values of deviations from the nominal value of the phase voltage of one of the phases of the electric motor. According to the hodograph diagrams of the Park vector, the values of the amplitudes of the stator phase currents and the phase shift angles between the current and voltage in each stator phase were calculated. The values of deviations of amplitudes and shifts in the angles of phase shift of the stator currents were calculated.

The amplitudes of the phase currents of the stator and the phase shift angles between the current and voltage in each phase of the stator were determined from the time diagrams of the stator currents. The values of deviations of amplitudes and shifts in the angles of phase shift of the stator currents were calculated. The error in calculating the values of deviations of amplitudes and displacements of the phase shift angles of the stator currents did not exceed 6%;

3. The Park vector hodograph was constructed under the condition of a fixed deviation from the nominal value of the phase voltage on one phase of the electric motor and

Symmetry **2022**, 14, 1305 32 of 34

a different number of working turns on one damaged stator phase. According to the hodograph diagrams of the Park vector, the values of the amplitudes of the stator phase currents and the phase shift angles between the current and voltage in each stator phase were calculated.

The amplitudes of the phase currents of the stator and the phase shift angles between the current and voltage in each phase were determined from the time diagrams of the stator currents. The values of deviations of amplitudes and displacements of phase shift angles of stator currents were calculated. The error in calculating the values of deviations of amplitudes and displacements of the phase shift angles of the stator currents did not exceed 6%;

- 4. The values of the amplitudes of the phase currents of the stator and the phase shift angles between the current and voltage in each phase, obtained in Paragraphs 2 and 3, were recalculated for the case of symmetry of the supply voltage system of the induction motor. The values of deviations of amplitudes and displacements of the phase shift angles of stator currents were calculated. The obtained results were compared with the results obtained in Paragraph 1. The error in calculating the values of deviations of the amplitudes and displacements of the phase shift angles of the stator currents did not exceed 6%;
- 5. The proposed algorithm makes it possible to determine, with high accuracy, the number of damaged turns of the stator winding, including in the presence of asymmetry of the supply voltage system of an induction motor.

The proposed method can be used in diagnosing other defects in an induction motor that cause an imbalance in the stator phase currents. Also, the proposed algorithm can be used in diagnosing a drive with induction motors, which are powered by an autonomous voltage inverter. Using the proposed method, it is possible to diagnose not only defects in an induction motor that cause an imbalance in the phase currents of the stator, but also defects in an autonomous voltage inverter.

**Author Contributions:** Conceptualization, S.G., J.G. and O.G.; methodology, J.G., S.G. and O.G.; software, S.G. and O.G.; validation, S.G., O.G. and A.T.; formal analysis, K.K., K.K.-S. and A.T.; investigation, J.G., S.G., O.G. and A.T.; resources, S.G., O.G. and A.T.; writing—original draft preparation, S.G., K.K. and K.K.-S.; writing—review and editing, J.G. and S.G.; visualization, O.G., K.K. and K.K.-S.; supervision, J.G. and S.G. All authors have read and agreed to the published version of the manuscript.

**Funding:** This publication was issued thanks to support from the Cultural and Educational Grant Agency of the Ministry of Education of the Slovak Republic in the projects, "Implementation of modern methods of computer and experimental analysis of properties of vehicle components in the education of future vehicle designers" (Project No. KEGA 036ŽU-4/2021). This research was also supported by the Slovak Research and Development Agency of the Ministry of Education, Science, Research and Sport of the Slovak Republic in Educational Grant Agency of the Ministry of Education of the Slovak Republic in the project and VEGA 1/0513/22 "Investigation of the properties of railway brake components in simulated operating conditions on a flywheel brake stand".

**Institutional Review Board Statement:** Not applicable.

**Data Availability Statement:** Not applicable.

**Conflicts of Interest:** The authors declare no conflict of interest.

## References

- 1. Turpak, S.M.; Taran, I.O.; Fomin, O.V.; Tretiak, O.O. Logistic technology to deliver raw material for metallurgical production. *Sci. Bull. Natl. Min. Univ.* **2018**, *1*, 162–169. Available online: http://nbuv.gov.ua/UJRN/Nvngu\_2018\_1\_2 (accessed on 20 February 2022). [CrossRef]
- 2. Klimenko, I.V.; Kalivoda, J.; Neduzha, L.O. Parameter Optimization of the Locomotive Running Gear. In Proceedings of the 22nd International Scientific Conference (Transport Means 2018), Trakai, Lithuania, 3–5 October 2018; pp. 1095–1098. Available online: http://eadnurt.diit.edu.ua/jspui/handle/123456789/10779 (accessed on 18 March 2022).

Symmetry **2022**, *14*, 1305 33 of 34

3. Lunys, O.; Neduzha, L.O.; Tatarinova, V.A. Stability Research of the Main-Line Locomotive Movement. In Proceedings of the 22nd International Scientific Conference (Transport Means 2019), Palanga, Lithuania, 2–4 October 2019; pp. 1341–1345. Available online: http://eadnurt.diit.edu.ua/jspui/handle/123456789/11520 (accessed on 18 March 2022).

- 4. Bondarenko, I.; Keršys, R.; Neduzha, L. Studying of Dynamic Parameters Impulse Impact of the Vehicle Taking into Account the Track Stiffness Variations. In Proceedings of the 25th International Conference (Transport Means 2021), Kaunas, Lithuania, 6–8 October 2021; Part II, pp. 684–689.
- 5. Píštěk, V.; Kučera, P.; Fomin, O.; Lovska, A. Effective mistuning identification method of integrated bladed discs of marine engine turbochargers. *J. Mar. Sci. Eng.* **2020**, *8*, 379. [CrossRef]
- 6. Fomin, O.; Lovska, A. Determination of dynamic loading of bearing structures of freight wagons with actual dimensions. *East.-Eur. J. Enterp. Technol.* **2021**, *2*, 6–14. [CrossRef]
- 7. Bodnar, B.; Ochkasov, O.; Bodnar, E.; Hryshechkina, T.; Keršys, R. Safety performance analysis of the movement and operation of locomotives. In Proceedings of the 22nd International Scientific Conference (Transport Means 2018), Trakai, Lithuania, 3–5 October 2018; Kaunas University of Technology: Kaunas, Lithuania, 2018; Part II, pp. 839–843, Prieiga per internet. Available online: <a href="https://transportmeans.ktu.edu/wp-content/uploads/sites/307/2018/02/Transport-means-II-A4-2018-09-25.pdf">https://transportmeans.ktu.edu/wp-content/uploads/sites/307/2018/02/Transport-means-II-A4-2018-09-25.pdf</a> (accessed on 20 April 2022).
- 8. Leitner, B.; Rehak, D.; Kersys, R. The new procedure for identification of infrastructure elements significance in sub-sector railway transport. *Commun.-Sci. Lett. Univ. Zilina* **2018**, 20, 41–48. [CrossRef]
- 9. Ocampo-Martinez, C. Energy efficiency in discrete-manufacturing systems: Insights, trends, and control strategies. *J. Manuf. Syst.* **2019**, 52, 131–145. [CrossRef]
- Fernandes, T.; Oliveira, E. Understanding consumers' acceptance of automated technologies in service encounters: Drivers of digital voice assistants adoption. J. Bus. Res. 2021, 122, 180–191. [CrossRef]
- 11. Yatsko, S.; Sidorenko, A.; Vashchenko, Y.; Liubarskyi, B.; Yeritsyan, B. Method to improve the efficiency of the traction rolling stock with onboard energy storage. *Int. J. Renew. Energy Researc.* **2019**, *2*, 1–11. Available online: https://www.ijrer.org/ijrer/index.php/ijrer/article/view/9143/pdf (accessed on 20 April 2022).
- 12. Dmitrienko, V.; Noskov, V.; Zakovorotniy, A.; Mezentsev, N.; Leonov, S.; Gasanov, M. Proactive Control of Rolling Stock with Traction Asynchronous Electric Motors. In Proceedings of the 2021 IEEE 2nd KhPI Week on Advanced Technology (KhPIWeek), Kharkiv, Ukraine, 13–17 September 2021; IEEE: New York, NY, USA, 2021; pp. 407–411. [CrossRef]
- 13. Tuychieva, M. Control of electric locomotives with asynchronous electric motors under asymmetric operating conditions in Uzbekistan. In Proceedings of the IOP Conference Series: Earth and Environmental Science, Tashkent, Uzbekistan, 14–16 October 2020; IOP Publishing: Bristol, UK, 2020; Volume 614, p. 012060. [CrossRef]
- Hiware, R.S.; Umathe, S.K.; Bire, S. Design of Sine Filter for GTO-Based Auxiliary Converter for Electric Locomotive Using MATLAB Simulink. In Smart Technologies for Energy. Environment and Sustainable Development; Springer: Singapore, 2022; Volume 2, pp. 561–569. [CrossRef]
- 15. Suresh, H.; Vaibhav, A.M.; Suresh, H.N. Power converters for three phase electric locomotives. *Linguist. Cult. Rev.* **2021**, *5*, 1083–1092. [CrossRef]
- 16. Ammar, N.R.; Seddiek, I.S. Evaluation of the environmental and economic impacts of electric propulsion systems onboard ships: Case study passenger vessel. *Environ. Sci. Pollut. Res.* **2021**, *28*, 37851–37866. [CrossRef]
- 17. Nguyen, H.P.; Hoang, A.T.; Nizetic, S.; Nguyen, X.P.; Le, A.T.; Luong, C.N.; Chu, V.D.; Pham, V.V. The electric propulsion system as a green solution for management strategy of CO<sub>2</sub> emission in ocean shipping: A comprehensive review. *Int. Trans. Electr. Energy Syst.* **2021**, *31*, e12580. [CrossRef]
- 18. Gundewar, S.K.; Kane, P.V. Condition monitoring and fault diagnosis of asynchronous motor. *J. Vib. Eng. Technol.* **2021**, *9*, 643–674. [CrossRef]
- 19. Liu, Y.; Cheng, Y.; Zhang, Z.; Wu, J. Multi-information Fusion Fault Diagnosis Based on KNN and Improved Evidence Theory. *J. Vib. Eng. Technol.* **2021**, *10*, 1–12. [CrossRef]
- 20. Soother, D.K.; Daudpoto, J. A brief review of condition monitoring techniques for the asynchronous motor. *Trans. Can. Soc. Mech. Eng.* **2019**, 43, 499–508. [CrossRef]
- 21. He, L.; Kang, J.; Li, H. An Interturn Short Circuit Fusion Model of Traction Motors for Fault Diagnosis. In Proceedings of the 2021 IEEE 1st International Power Electronics and Application Symposium (PEAS), Shanghai, China, 13–15 November 2021; IEEE: New York, NY, USA, 2021; pp. 1–5. [CrossRef]
- 22. Goolak, S.; Tkachenko, V.; Bureika, G.; Vaičiūnas, G. Method of spectral analysis of traction current of AC electric locomotives. *Transport* **2020**, *35*, 658–668. [CrossRef]
- 23. Goolak, S.; Gerlici, J.; Gubarevych, O.; Lack, T.; Pustovetov, M. Imitation Modeling of an Inter–Turn Short Circuit of an Asynchronous Motor Stator Winding for Diagnostics of Auxiliary Electric Drives of Transport Infrastructure. *Commun.-Sci. Lett. Univ. Zilina* 2021, 23, C65–C74. [CrossRef]
- 24. Gubarevych, O.; Goolak, S.; Daki, O.; Tryshyn, V. Investigation of Turn-To-Turn Closures of Stator Windings to Improve the Diagnostics System for Asynchronous motors. *Probl. Energet. Reg.* **2021**, *2*, 10–24. [CrossRef]
- 25. Goolak, S.; Tkachenko, V.; Šťastniak, P.; Sapronova, S.; Liubarskyi, B. Analysis of Control Methods for the Traction Drive of an Alternating Current Electric Locomotive. *Symmetry* **2022**, *14*, 150. [CrossRef]

Symmetry **2022**, *14*, 1305 34 of 34

26. Tian, Y.; Guo, D.; Zhang, K.; Jia, L.; Qiao, H.; Tang, H. A review of fault diagnosis for traction asynchronous motor. In Proceedings of the 2018 37th Chinese Control Conference (CCC), Wuhan, China, 25–27 July 2018; IEEE: New York, NY, USA, 2018; pp. 5763–5768. [CrossRef]

- 27. Gubarevych, O.; Goolak, S.; Daki, O.; Yakusevych, Y. Determining an additional diagnostic parameter for improving the accuracy of assessment of the condition of stator windings in an asynchronous motor. *East.-Eur. J. Enterp. Technol.* **2021**, *5*, 21–29. [CrossRef]
- 28. Asad, B.; Vaimann, T.; Belahcen, A.; Kallaste, A. Broken rotor bar fault diagnostic of inverter fed asynchronous motor using FFT, Hilbert and Park's vector approach. In Proceedings of the 2018 XIII International Conference on Electrical Machines (ICEM), Alexandroupoli, Greece, 3–6 September 2018; IEEE: New York, NY, USA, 2018; pp. 2352–2358. [CrossRef]
- 29. Guefack, F.L.T.; Kiselev, A.; Kuznietsov, A. Improved detection of inter-turn short circuit faults in PMSM drives using principal component analysis. In Proceedings of the 2018 International Symposium on Power Electronics, Electrical Drives, Automation and Motion (SPEEDAM), Amalfi, Italy, 20–22 June 2018; IEEE: New York, NY, USA, 2018; pp. 154–159. [CrossRef]
- 30. Sha, M.; Luo, M. Online Identification Technology Based on Variation Mechanism of Traction Motor Parameters. In Proceedings of the 2021 4th International Conference on Advanced Electronic Materials, Computers and Software Engineering (AEMCSE), Changsha, China, 26–28 March 2021; IEEE: New York, NY, USA, 2021; pp. 77–82. [CrossRef]
- 31. Gonzalez-Jimenez, D.; del-Olmo, J.; Poza, J.; Garramiola, F.; Sarasola, I. Machine Learning-Based Fault Detection and Diagnosis of Faulty Power Connections of Induction Machines. *Energies* **2021**, *14*, 4886. [CrossRef]
- 32. Goolak, S.; Liubarskyi, B.; Sapronova, S.; Tkachenko, V.; Riabov, I. Refined Model of Asynchronous Traction Electric Motor of Electric Locomotive. In Proceedings of the 25th International Science Conference (Transport Means 2021), Kaunas, Lithuania, 6–8 October 2021; IEEE: New York, NY, USA, 2021; Part I, pp. 455–460.
- 33. Goolak, S.; Liubarskyi, B.; Sapronova, S.; Tkachenko, V.; Riabov, I.; Glebova, M. Improving a Model of the Induction Traction Motor Operation Involving Non-Symmetric Stator Windings. *East.-Eur. J. Enterp. Technol.* **2021**, *4*, 112. [CrossRef]
- 34. Goolak, S.; Gerlici, J.; Tkachenko, V.; Sapronova, S.; Lack, T.; Kravchenko, K. Determination of parameters of asynchronous electric machines with asymmetrical windings of electric locomotives. *Commun.-Sci. Lett. Univ. Zilina* **2019**, *21*, C24–C31. [CrossRef]
- 35. Merabet, H.; Bahi, T.; Bedoud, K.; Drici, D. Real-Time Switches Fault Diagnosis for Voltage Source Inverter Driven Asynchronous motor Drive. *Int. J. Electr. Electron. Eng. Telecommun.* **2019**, *8*, 103–107. [CrossRef]
- 36. Wang, W.; Liu, C.; Liu, S.; Zhao, H. Model predictive torque control for dual three-phase PMSMs with simplified deadbeat solution and discrete space-vector modulation. *IEEE Trans. Energy Convers.* **2021**, *36*, 1491–1499. [CrossRef]
- 37. Amanuel, T.; Ghirmay, A.; Ghebremeskel, H.; Ghebrehiwet, R. and Bahlibi, W. Design of Vibration Frequency Method with Fine-Tuned Factor for Fault Detection of Three Phase Asynchronous motor. J. Innov. Image Process. (JIIP) 2021, 3, 52–65. [CrossRef]
- 38. Balakin, A.V.; Garnov, S.V.; Makarov, V.A.; Kuzechkin, N.A.; Obraztsov, P.A.; Solyankin, P.M.; Shkurinov, A.P.; Zhu, Y. "Terhune-like" transformation of the terahertz polarization ellipse "mutually induced" by three-wave joint propagation in liquid. *Opt. Lett.* **2018**, 43, 4406–4409. [CrossRef]
- 39. Gil, J.J.; Norrman, A.; Friberg, A.T.; Setälä, T. Nonregularity of three-dimensional polarization states. *Opt. Lett.* **2018**, 43, 4611–4614. [CrossRef]
- 40. Gil, J.J.; Norrman, A.; Friberg, A.T.; Setälä, T. Polarimetric purity and the concept of degree of polarization. *Phys. Rev. A* **2018**, 97, 023838. [CrossRef]
- 41. Dyks, J.; Weltevrede, P.; Ilie, C. Circular polarization in radio pulsar PSR B1451–68: Coherent mode transitions and intrabeam interference. *Mon. Not. R. Astron. Soc.* **2021**, *501*, 2156–2173. [CrossRef]
- 42. Golden, R.; Delanois, J.E.; Sanda, P.; Bazhenov, M. Sleep prevents catastrophic forgetting in spiking neural networks by forming joint synaptic weight representations. *bioRxiv* **2020**. bioRxiv:688622. [CrossRef]
- 43. Pei, J.; Zou, M.; Zhao, Y. Adaptive comb-type filtering method for stripe noise removal in infrared images. *J. Electron. Imaging* **2019**, *28*, 013037. [CrossRef]
- 44. Alloui, A.; Laadjal, K.; Sahraoui, M.; Cardoso, A.J.M. Online Inter-Turn Short-Circuit Fault Diagnosis in Induction Motors Operating Under Unbalanced Supply Voltage and Load Variations, Using the STLSP Technique. *IEEE Trans. Ind. Electron.* 2022, 1–10. [CrossRef]
- 45. Rajamany, G.; Rajamany, K.; Natarajan, R.K. Negative Sequence Current Compensation for Induction Motor Stator Inter-Turn Short Circuit and Off-Diagonal Term in Sequence Impedance Matrix as Fault Indicator. *J. Electr. Eng. Technol.* **2021**, *16*, 2075–2082. [CrossRef]
- 46. Tomczyk, M.; Mielnik, R.; Plichta, A.; Goldasz, I.; Sułowicz, M. Identification of Inter-Turn Short-Circuits in Induction Motor Stator Winding Using Simulated Annealing. *Energies* **2021**, *15*, 117. [CrossRef]
- 47. Dolgih, R.; Suvorov, I.; Palkin, G.; Kakaurov, S.; Morozova, M. Development of the software-hardware complex for diagnostics of inter-turn short circuits of stator windings of asynchronous motors. In Proceedings of the E3S Web of Conferences, 2021, EDP Sciences, Kazan, Russia, 18–20 February 2021; Volume 288, p. 01040. [CrossRef]